Journal of Vertebrate Paleontology

ISSN: 0272-4634 (Print) 1937-2809 (Online) Journal homepage: www.tandfonline.com/journals/ujvp20

An early to middle Uintan (Ui1b–Ui2) mammalian fauna from the upper unit of the middle Eocene Adobe Town Member, Washakie Formation (Wyoming, U.S.A.)

Steven M. McCarroll, Susumu Tomiya, Rachel H. Dunn, Shawn P. Zack, Melissa C. Wood, Bin Bai, William D. Turnbull & John J. Flynn

To cite this article: Steven M. McCarroll, Susumu Tomiya, Rachel H. Dunn, Shawn P. Zack, Melissa C. Wood, Bin Bai, William D. Turnbull & John J. Flynn (2025) An early to middle Uintan (Ui1b–Ui2) mammalian fauna from the upper unit of the middle Eocene Adobe Town Member, Washakie Formation (Wyoming, U.S.A.), Journal of Vertebrate Paleontology, 45:4, e2570730, DOI: 10.1080/02724634.2025.2570730

To link to this article: https://doi.org/10.1080/02724634.2025.2570730

Journal of Vertebrate Paleontology e2570730 (20 pages)

DOI: 10.1080/02724634.2025.2570730

ARTICLE

AN EARLY TO MIDDLE UINTAN (UI1B–UI2) MAMMALIAN FAUNA FROM THE UPPER UNIT OF THE MIDDLE EOCENE ADOBE TOWN MEMBER, WASHAKIE FORMATION (WYOMING, U.S.A.)

STEVEN M. MCCARROLL,[1†] SUSUMU TOMIYA, [1,2,3*] RACHEL H. DUNN, [4] SHAWN P. ZACK, [5,6] MELISSA C. WOOD, [7] BIN BAI, [8] WILLIAM D. TURNBULL,[1†] and JOHN J. FLYNN [1,9]

[1]Field Museum of Natural History, Chicago, Illinois 60605, U.S.A.;
[2]Center for International Collaboration and Advanced Studies in Primatology, Center for the Evolutionary Origins of Human Behavior, Kyoto University, Inuyama, Aichi 484-8506, Japan, tomiya.susumu.8r@kyoto-u.ac.jp;
[3]University of California Museum of Paleontology, Berkeley, California 94720, U.S.A.;
[4]Department of Anatomy, Des Moines University, West Des Moines, Iowa 50266, U.S.A., rachel.dunn@dmu.edu;
[5]Department of Basic Medical Sciences, University of Arizona College of Medicine-Phoenix, Phoenix, Arizona 85004, U.S.A.;
[6]School of Human Evolution and Social Change, Arizona State University, Tempe, Arizona 85281, U.S.A., zack@arizona.edu;
[7]Department of Geophysical Sciences, University of Chicago, Chicago, Illinois 60637, U.S.A., melissawood@uchicago.edu;
[8]Key Laboratory of Vertebrate Evolution and Human Origins, Institute of Vertebrate Paleontology and Paleoanthropology, Chinese Academy of Sciences, Beijing, China, baibin@ivpp.ac.cn;
[9]Division of Paleontology and Richard Gilder Graduate School, American Museum of Natural History, New York, New York 10024, U.S.A., jflynn@amnh.org

ABSTRACT—The mammalian fossil record of the middle Eocene Washakie Formation of Wyoming, U.S.A., has provided important insights into both climatic (cooling and drying) and associated biotic changes during an early phase of the Eocene–Oligocene transition within a single depositional basin. However, only provisional assessments of the biochronological age of its uppermost unit, Twka3 of the Adobe Town Member, have been made, without formal description of most of the fossil material from there. Here we document all mammalian specimens that are currently known from Twka3 and can be identified at the taxonomic level of suborder or below. They represent 12 taxa of Cimolesta, Primates, Rodentia, Hyaenodonta, Carnivoramorpha, Artiodactyla, and Perissodactyla. Based on the updated taxon occurrence data, we propose an early to middle Uintan (Ui1b–Ui2) North American Land Mammal 'Age' for the lower part of Twka3. Although the fossil mammal sample from Twka3 is much smaller than those from the underlying upper Bridgerian to lower Uintan (Br3–Ui1b) aged units of the Adobe Town Member, it enhances the resolution of faunal transition data for the middle Eocene of the central Rocky Mountain region, uniquely contributing to our understanding of regional mammalian diversity dynamics against the backdrop of contracting lake systems and climate-driven cooling and drying. Recovery of primate and pantolestid material in this small sample is surprising given their virtual absence in the much better-sampled lower Uintan (Ui1b) portion of the underlying Twka2, hinting at complexity of the local environmental history within a broader regional trend of contracting lake systems and forests.

SUPPLEMENTARY FILES—Supplementary files are available for this article for free at www.tandfonline.com/UJVP.

Citation for this article: McCarroll, S. M., Tomiya, S., Dunn, R. H., Zack, S. P., Wood, M. C., Bai, B., Turnbull, W. D., & Flynn, J. J. (2025) An early to middle Uintan (Ui1b–Ui2) mammalian fauna from the upper unit of the middle Eocene Adobe Town Member, Washakie Formation (Wyoming, U.S.A.). *Journal of Vertebrate Paleontology.* https://doi.org/10.1080/02724634.2025.2570730

Submitted: January 29, 2025
Revisions received: September 9, 2025
Accepted: September 18, 2025
First published online: November 21, 2025

INTRODUCTION

Since the early 20th century, the age of the Washakie Formation in the Washakie Basin, Wyoming, U.S.A. (Fig. 1), has been investigated with increasing stratigraphic, faunal, and temporal resolution (Flynn, 1986; Granger, 1909; McCarroll et al., 1996a; Murphey et al., 2018; Roehler, 1973, 1992; Turnbull, 1972, 1978; Tsukui et al., 2025). These attempts varied with the available data and in their rigor. We here further refine the biochronological age of the Washakie Formation, specifically the age of the lower part of the uppermost unit of the Adobe Town Member (henceforth abbreviated as Twka3).

The Washakie Formation was named by Granger (1909), who divided it into two lithostratigraphic units, horizons A (below) and B (above). Washakie A and Washakie B were faunally correlated with the upper Bridger Formation (Bridger C–D) of the Bridger Basin, Wyoming, and the lower Uinta Formation (Uinta A–B) of the Uinta Basin, Utah, respectively. Thus, it

*Corresponding author.
†Deceased
Color versions of one or more of the figures in the article can be found online at www.tandfonline.com/ujvp.

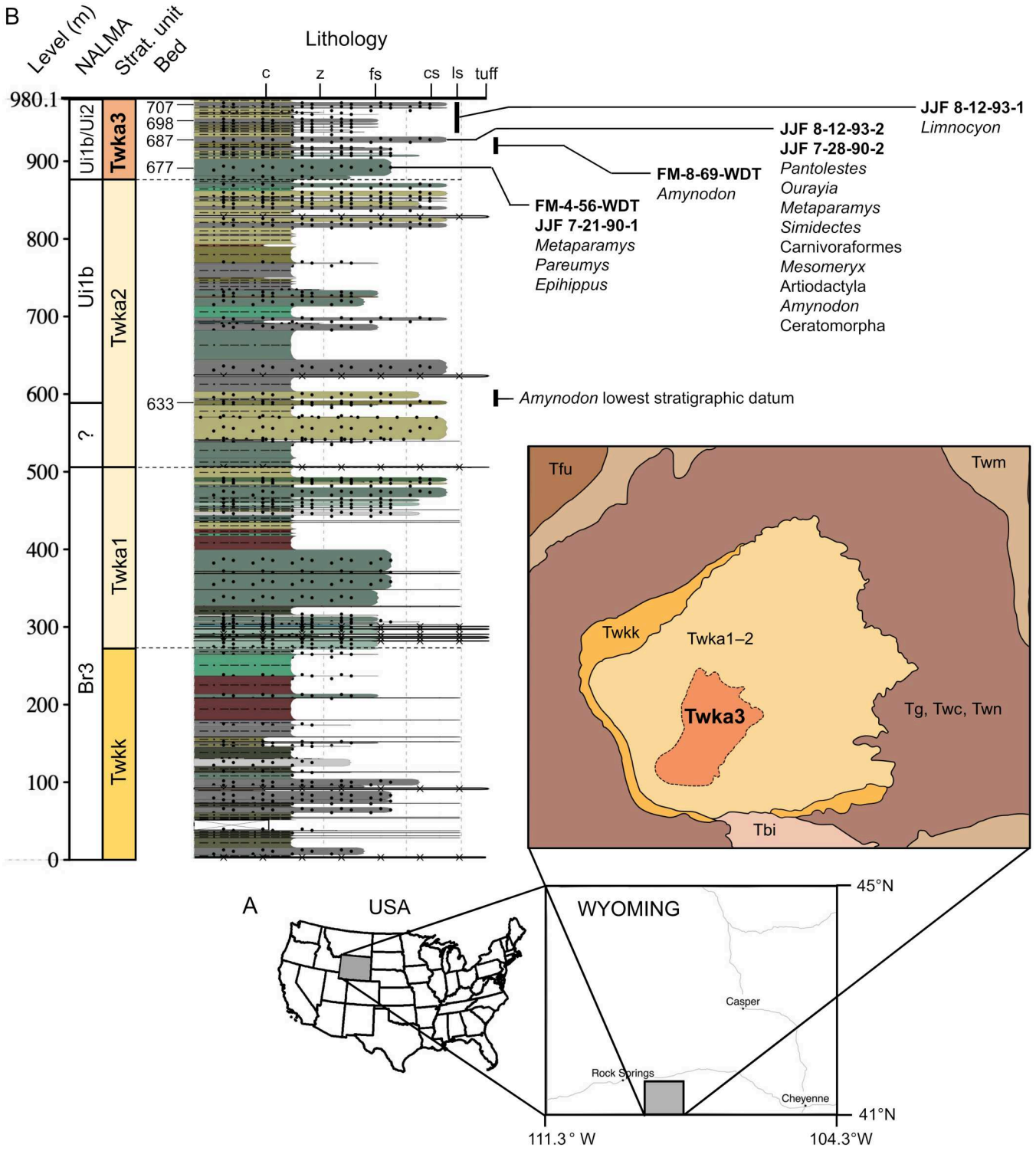

FIGURE 1. Geographic and geologic context. **A**, general location map showing geographic location of the Washakie Basin. Detailed map of study area showing outcrop extent of the Washakie Formation members and underlying stratigraphic units. Modified from Scott et al. (2011), Love and Christiansen (1985), and Roehler (1985). **B**, composite stratigraphic column based on Roehler's (1973) descriptions of the type section of Twkk and principal reference sections of Twka. Approximate horizons corresponding to fossil-producing Twka3 localities are marked. **Abbreviations**: **c**, clay; **cs**, coarse sand; **fs**, fine sand; **ls**, limestone; **Tbi**, Bishop Conglomerate; **Twc**, Wasatch Formation, Cathedral Bluffs Tongue; **Tfu**, Fort Union Formation; **Tg**, Green River Formation; **Twkk**, Washakie Formation, Kinney Rim Member; **Twka1–2**, Washakie Formation, Adobe Town Member, lower and middle units; **Twka3**, Washakie Formation, Adobe Town Member, upper unit; **Twm**, Wasatch Formation, main body; **Twn**, Wasatch Formation, Niland Tongue (from Love and Christiansen, 1985); **z**, silt.

can be inferred that the Washakie Formation spans two successive North American Land Mammal 'Ages' (NALMAs)—the Bridgerian and the Uintan.

Although the Bridgerian/Uintan boundary is now recognized within the Bridger Formation, Wyoming (Kelly & Murphey, 2016; Murphey et al., 2018; Murphey & Kelly, 2017), the extent of the faunal turnover between the Bridgerian and Uintan ages is not adequately preserved in any single rock formation in North America other than the Washakie Formation, making the latter central to understanding an early phase of the Eocene–Oligocene biotic transition (cf. McCarroll et al., 1996a; Tomiya et al., 2021) under multi-million-year trends of global cooling (Zachos et al., 2001), drying, and contraction of lake systems in the region (Smith et al., 2008) across the middle to late Eocene.

Roehler (1973) further divided the Washakie Formation into formal lithologic units. He was the first to recognize that what was then the upper portion of the Laney Shale Member of the Green River Formation directly underlying the Washakie Formation was lithologically more like the Washakie Formation than the Green River Formation, being predominantly fluvial rather than lacustrine, as is more typical for the Green River Formation. Roehler (1973) named these rocks the Kinney Rim Member (Twkk) of the Washakie Formation. The Kinney Rim Member conformably overlies the Green River Formation via the White Ridge Marker bed (Roehler's [1973] bed 515), and unconformably underlies the Lower Brown Sandstone (bed 569; the basal bed of the Adobe Town Member). The Kinney Rim Member was assigned an early Bridgerian age based on a small fauna (Turnbull, 1972; ~bed 533) and on stratigraphic correlations (Roehler 1973). On the basis of perissodactyls, however, McCarroll et al. (1996b) revised that assessment and proposed a late Bridgerian (essentially biochron Br3 of Gunnell et al. [2009]) age for it. Formal description of the mammalian assemblage of Twkk, enhanced by stratigraphically controlled collecting of additional fossils in recent years by one of us (M.C.W.), is currently underway.

Roehler (1973) assigned the remaining Washakie Formation (i.e., all of the Washakie Formation as conceived earlier) to the Adobe Town Member, which he divided into three informal units: lower, middle, and upper. The lower unit is equivalent to Granger's (1909) Washakie A (beds 569–619), and the middle unit to his Washakie B (beds 620–675). Turnbull (1978) further designated them as Twka1 and Twka2. While it had long been assumed that the topographically highest beds (i.e., those that cap Haystack Mountain; beds 661–675) were also the stratigraphically highest beds in the formation (Granger 1909), Turnbull (1972, 1978) and Roehler (1973) independently recognized that there was an additional series of beds (676–708) in the geographic center of the basin. These beds were designated as the upper Adobe Town Member, or Twka3 (Roehler, 1973; Turnbull, 1978). No obvious unconformity has been detected between the Twka3 and the underlying Twka2. Unit Twka3 was conjectured to correlate with the Uinta C horizon (i.e., the Myton Member of the Uinta Formation), implying a late Uintan age, on the basis of a shift in lithology from the underlying beds (Roehler, 1973), but without a biostratigraphic analysis. It is worth noting that although the lithostratigraphic division of Twka1 and Twka2 via bed 620 has often been used to approximate the Bridgerian/Uintan boundary, the lower portion of Twka2 is thus far lacking mammalian taxa that are indicative of the Uintan NALMA (cf. Tomiya et al., 2021). As such, the lithologic boundary between Twka1 and Twka2 should be considered independent from any faunal transition.

Since then, the vertebrate fossil sample from Twka3 grew in size through intensive collecting efforts led by W.D. Turnbull and J.J. Flynn of the Field Museum of Natural History, although the upper part of the unit (beds 689–708) has not yielded enough diagnostic specimens for robust faunal correlation. The next synthesis of the mammalian biostratigraphy of the Washakie Formation including Twka3 was published by McCarroll et al. (1996a), building on an earlier work by Flynn (1986) that correlated major middle Eocene formations of western North America. McCarroll et al. (1996a) revised the mammalian faunal list for the Washakie Formation and suggested an "early" rather than late Uintan age for Twka3 in reference to a tripartite division (earliest/early/late) of the Uintan NALMA (cf. Flynn, 1986; Krishtalka et al., 1987) and based on occurrence of the cylindrodontid rodent *Pareumys grangeri*, whose known distribution at that time was restricted to the Uinta B horizon (i.e., the Wagonhound Member) of the Uinta Formation. This work was cited by Robinson et al. (2004), who assigned, without elaborating, a middle (Ui2) or late Uintan (Ui3) age to Twka3, within an updated tripartite division of the Uintan NALMA (Ui1/Ui2/Ui3, or early/middle/late Uintan). Since then, the specimen underlying McCarroll et al.'s (1996a) age determination for Twka3, FMNH PM 55060, has been reidentified as belonging to a new species, *Pareumys flynni* (Korth, 2020), and the Uintan biochronology has been further refined to include the earliest (Ui1a), early (Ui1b), middle (Ui2), and late (Ui3) divisions (Murphey et al., 2018), necessitating reevaluation of the biochronologic age of Twka3.

At present, the only published mammalian specimens from Twka3 are those of the ischyromyid rodent *Metaparamys compressidens* (Korth, 1988, 2020; Korth & Emry, 2007; Wood, 1962), the cylindrodontid rodent *P. flynni* (Korth, 2020), and the equid perissodactyl *Epihippus gracilis* (McCarroll et al., 1996b). Four other taxa (the omomyid primate *Ourayia uintensis*, carnivoraform *Miacis* sp., homacodontid artiodactyl *Mesomeryx* cf. *M. grangeri*, and, questionably, amynodontid perissodactyl *Amynodon advenus*) were listed in the faunal table of McCarroll et al. (1996a), but the pertinent specimens have never been described in the literature. The three previously described species are unhelpful in resolving the precise age of Twka3, since *P. flynni* is thus far known only from the Washakie Formation, and the other two species occur across early to late Uintan (Ui1b–Ui3) aged rocks (Gunnell et al., 2009; Korth, 2020). Magnetostratigraphic polarity data are not available for Twka3, but based on Flynn's (1986) data, the underlying upper portion of Twka2 is currently thought to be correlative to Chron C20r (McCarroll et al., 1996a; Murphey et al., 2018; Smith et al., 2008; Tsukui et al., 2025), implying a maximum age of 45.57 Ma for Twka3 (cf. Tsukui & Clyde, 2012).

The present paper represents the "subsequent publication" on the mammalian assemblage of Twka3 mentioned by McCarroll et al. (1996a:31). Its early drafts were prepared starting in the 1990s by three of this study's authors (S.M.M., W.D.T., and J.J.F.), and a conference presentation on the topic was given by the lead author (McCarroll, 1995). After the deaths of two of the original authors (S.M.M. and W.D.T.), this study remained unpublished. Meanwhile, a renewed effort to curate the Washakie Formation vertebrate fossil collection at the Field Museum of Natural History (Chicago, IL, U.S.A.) commenced in 2013 (see Acknowledgments), augmenting the small yet paleontologically important sample of mammalian fossils from Twka3 and facilitating their description. In 2024, the remaining authors (S.T., R.H.D., S.P.Z., M.C.W., B.B., and J.J.F.) revised the last existing draft of the paper in light of the current taxonomy, systematics, and biostratigraphy and biochronological correlations.

MATERIALS AND METHODS

All Washakie Formation lithostratigraphic bed numbers are those of Roehler (1973, 1992). Unless otherwise stated, all

dental and anatomical measurements are in millimeters (mm). High-magnification digital photographs and original measurements were taken with digital calipers and Dino-Lite digital microscopes (DINOAM7915MZTL and DINOAM73915MZT; AnMo Electronics Corporation, New Taipei City, Taiwan), using an accompanying calibration slide and digital measurement tools of DinoCapture 2.0 imaging software. Digital photographs of small objects were focus-stacked via depth-map rendering ("Method B" with default parameter settings: radius = 8, smoothing = 4) in Helicon Focus version 8 (Helicon Soft Ltd, Kharkiv, Ukraine).

Author M.C.W. conducted stratigraphic fieldwork in the Washakie Formation, which included measurement and description of new sections through Twka3 and correlation of those sections with the principal reference sections from Roehler (1973). Measurements were taken using a Jacob's staff and correlations were made by tracing marker beds in outcrops and in satellite imagery. Author M.C.W. revisited many of the FMNH localities listed below and summarized in Table 1, including those mapped by Turnbull (1978). For those, bed assignments from original collection notes by W.D. Turnbull, J.J. Flynn, and S.M. McCarroll (digitally archived in the Geology Collections at FMNH) were corroborated via lithologic correlation in the field. Bed assignments of localities not revisited by M.C.W. were approximated by corroborating stratigraphic information from original collection notes (when available) with correlation of new sections and satellite imagery information.

A subset of specimens reported in this paper were imaged by means of X-ray computed tomography (XCT). The specimens were scanned at the Field Museum XCT Lab using an X25 Industrial CT Scanner (North Star Imaging, Inc., Rogers, MN, U.S.A.) with a 131 kV X-ray tube, with the focal spot size of 20 or 50 μm. Tomographic reconstruction was performed using the program efX-CT (proprietary software of the XCT scanner's manufacturer). Reconstructed slices were segmented in 3D Slicer version 5.8.1 (www.slicer.org). The reconstructed XCT slices and the digital 3D models along with documents summarizing additional, specimen-specific information on the XCT process are deposited on MorphoSource (see Data Availability Statement).

Institutional Abbreviations—**AMNH**, American Museum of Natural History, New York, NY, U.S.A.; **CM**, Carnegie Museum of Natural History, Pittsburgh, PA, U.S.A.; **FMNH**, Field Museum of Natural History, Chicago, IL, U.S.A.; **YPM**, Yale Peabody Museum, New Haven, CT, U.S.A.

Other Abbreviations—**L**, anteroposterior or mesiodistal length; **NALMA**, North American Land Mammal 'Age'; **Twka1/2/3**, lower/middle/upper unit of the Adobe Town Member, Washakie Formation; **Ui1a/Ui1b/Ui2/Ui3**, earliest/early/middle/late Uintan NALMA; **W**, labiolingual or buccolingual width.

TABLE 1. The FMNH Twka3 localities reported in this study. Approximate stratigraphic positions refer to Roehler's (1973) beds. Localities that have not yielded sufficiently identifiable mammalian fossils are not included.

Locality number	Stratigraphic position	Remarks
JJF 8-12-93-1	above bed 688	
JJF 7-28-90-2	~bed 687	
JJF 8-12-93-2	~bed 687	
FM-8-69-WDT	~bed 680–687	Mapped in Turnbull (1978:pl. 3).
JJF 7-21-90-1	~bed 677	Approximately equivalent to FM-4-56-WDT.
FM-4-56-WDT	~bed 677	Approximately equivalent to JJF 7-21-90-1. Mapped in Turnbull (1978:pl. 3).

SYSTEMATIC PALEONTOLOGY

Order CIMOLESTA McKenna, 1975
Suborder PANTOLESTA McKenna, 1975
Family PANTOLESTIDAE Cope, 1884
Genus *PANTOLESTES* Cope, 1872
PANTOLESTES cf. *P. LONGICAUDUS* Cope, 1872
(Fig. 2)

Referred Specimen—Locality JJF 8-12-93-2 (~bed 687): FMNH PM 56221, left M1.

Measurements—M1L = 4.48; M1W = 5.82.

Description—FMNH PM 56221 is tritubercular with a distinct cingular hypocone. A buccal cingulum with a weak ectoflexus is present, and the cingulum is slightly expanded anterior to the paracone, where there is a small, peripherally situated parastyle. A very small metastyle is present posterior to the metacone. The protocone is the largest of the main cusps, with distinct preprotocrista and postprotocrista. A distinct metaconule is present as a swelling on the postprotocrista lingual to the metacone. A paraconule is present on the preprotocrista, being smaller and positioned slightly more lingually than the metaconule. The metacone is smaller than the paracone and situated somewhat more lingually. The paracone and metacone are joined by a low centrocrista. The hypocone is developed from the posterolingual cingulum, posterior and lingual to the protocone. A small anterolingual cingulum is present near the base of the tooth, separate from the buccal cingulum.

Comments—*Pantolestes* is common in the lower unit of the Adobe Town Member (Twka1), and appears to be represented by three distinct species, two smaller and one larger. *Pantolestes* is represented in the middle unit (Twka2) by one species, but is rare there. The present report extends the stratigraphic distribution of pantolestids within the Washakie Formation to include Twka3, hence the family now is represented throughout the Adobe Town Member.

Pantolestids are documented in North America from the Wasatchian through the Chadronian, although they decrease in abundance after the Bridgerian. Two species of Uintan pantolestids are known from the Ui2 and Ui3 intervals of the Uinta Formation, Utah, both members of the genus *Pantolestes*. Dunn and Townsend (2019) attributed the larger of the two Uintan species to the previously known Bridgerian species *P. natans* Matthew, 1909, based on overall similarity in morphology and size. The smaller Uintan species is more problematic. Although these specimens were consistently larger than the Bridgerian *P. longicaudus*, there are no known morphological characteristics that distinguish them, and their molar dimensions sometimes overlap. That, combined with the relatively small sample size, led the authors to refer the smaller Uintan species to *P. longicaudus*, pending better material and more convincing diagnostic criteria. FMNH PM 56221 compares well in size and morphology with Uintan *P. longicaudus* described by Dunn and Townsend (2019) and is intermediate in size between the small and large *Pantolestes* specimens from Twka1. For that reason, we tentatively assign this specimen to *Pantolestes* cf. *P. longicaudus*. Specimens that likely represent *P. longicaudus* also occur in Twka2 (FMNH PM 60694, FMNH PM 61333), and will be described elsewhere along with pantolestids from Twka1.

Order PRIMATES Linnaeus, 1758
Family OMOMYIDAE Trouessart, 1879
Genus *OURAYIA* Gazin, 1958
OURAYIA UINTENSIS (Osborn, 1895)
(Figs. 3, S1, S2)

Referred Specimens—Locality JJF 8-12-93-2 (~bed 687): FMNH PM 56654, right m3; FMNH PM 56655, right m2.

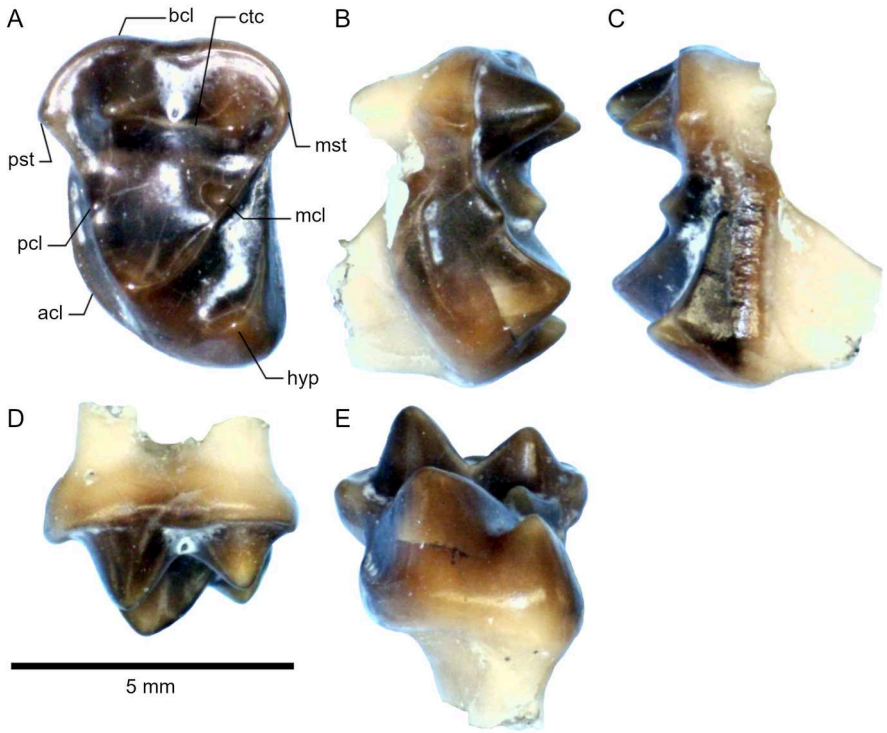

FIGURE 2. Pantolestidae. Specimen FMNH PM 56221 (*Pantolestes* cf. *P. longicaudus*): left M1 in occlusal, **A**, anterior, **B**, posterior, **C**, buccal, **D**, and lingual, **E** views. **Abbreviations**: **acl**, anterolingual cingulum; **bcl**, buccal cingulum; **ctc**, centrocrista; **hyp**, hypocone; **mcl**, metaconule; **mst**, metastyle; **pcl**, paraconule; **pst**, parastyle.

Measurements—FMNH PM 56654: m3L = 4.60; m3W = 3.05. FMNH PM 56655: m2L = 3.78; m2W = 3.39.

Description—Specimen FMNH PM 56654 is a lightly worn right m3. It exhibits crenulated enamel, especially in the talonid basin (Fig. 3B, D). The trigonid is only moderately elevated above the talonid (Fig. 3H). The cuspids are low and bunodont. A small paraconid is present, situated approximately midway between the protoconid and metaconid, and is connected to each of those cuspids by a rounded paracristid. The metaconid and protoconid are connected by a low, V-shaped (in posterior view) protocristid. The talonid is slightly wider than the trigonid (not including the buccal cingulid), and possesses an expanded hypoconulid lobe. A buccal cingulid extends from the anterobuccal corner of the tooth to the hypoconid.

Specimen FMNH PM 56655 is a heavily worn right m2. Its anterior and posterior borders are flat and show considerable interdental wear (Fig. 3A, C, E, G). The trigonid cuspids are all worn down to their bases, but it appears that a small paraconid was present and situated anterior and slightly buccal to the metaconid. All three trigonid cuspids are represented by two large dentine pools, which are anteriorly connected by a narrow bridge of dentine representing a paracristid. An enamel island is present on the posterior trigonid between the paraconid and metaconid, suggesting that the trigonid was open posteriorly. Lingually, the trigonid appears elongate, suggesting the presence of a postmetacristid in the unworn tooth. A gap between the posterior aspect of the metaconid and the anterior aspect of the entoconid suggests that the talonid was open lingually. The talonid is wider than the trigonid and preserves a small, centrally located hypoconulid along the hypocristid that joins the hypoconid and entoconid. Similar to the trigonid, all three main talonid cuspids are worn down to a continuous dentine pool. A buccal cingulid is present and extends from anterior to the protoconid to the hypoconid. A small posterobuccal cingulid is also present near the base of the tooth, slightly buccal to the hypoconulid.

Comments—*Hemiacodon gracilis* Marsh, 1872b, is the most common omomyid primate in the lower unit of the Adobe Town Member (Twka1). The diminutive genus *Omomys* Leidy, 1869a, is also present, although it is rare. The lower molars of *Ourayia* differ from those of *Hemiacodon* Marsh, 1872b, in having more bunodont cuspids, with anteriorly restricted cingulids, a more rounded cristid obliqua that meets the posterior trigonid more buccally, and in being larger on average, although there is size overlap between the two taxa (Kirk et al., 2023; Szalay, 1976); FMNH PM 56654 falls within the known size range of *O. uintensis*, and is larger than any *Hemiacodon* m3 from the Washakie Basin; although it is only slightly longer, it is significantly wider. When specimens of *Hemiacodon* from the Bridger Formation are considered, FMNH PM 56654 falls within the upper range for *H. gracilis* and *H. engardae* Murphey and Dunn, 2009, but it is, again, significantly wider than specimens of those taxa. It can be distinguished from *Mytonius* Robinson, 1968, in being anteroposteriorly longer, with an expanded talonid basin and wider hypoconulid lobe, and having a less anteroposteriorly compressed trigonid basin (Kirk et al., 2023). FMNH PM 56654 is slightly smaller than m3s of *Macrotarsius* Clark, 1941, and lacks the development of shearing crests present in that genus (Kirk et al., 2023; Szalay, 1976). In sum, FMNH PM 56654 best fits the range of m3 morphology seen in *Ourayia uintensis* (Fig. S1).

The advanced state of wear makes identification of FMNH PM 56655 more problematic. In size, this tooth is within the upper limit of *H. gracilis* in anteroposterior length but outside the range in width (Murphey & Dunn, 2009; Szalay, 1976). Specimen FMNH PM 56655 is slightly shorter in length than m2s of *O. uintensis* reported by Kirk et al. (2023) but within the ranges reported by Szalay (1976) and is well within the published ranges of m2 widths (Kirk et al., 2023; Szalay, 1976) and m2 areas (Kirk et al. 2023). Because of the substantial wear and breakage, especially on the anterior aspect of the tooth, our m2L measurement likely underestimates the original length.

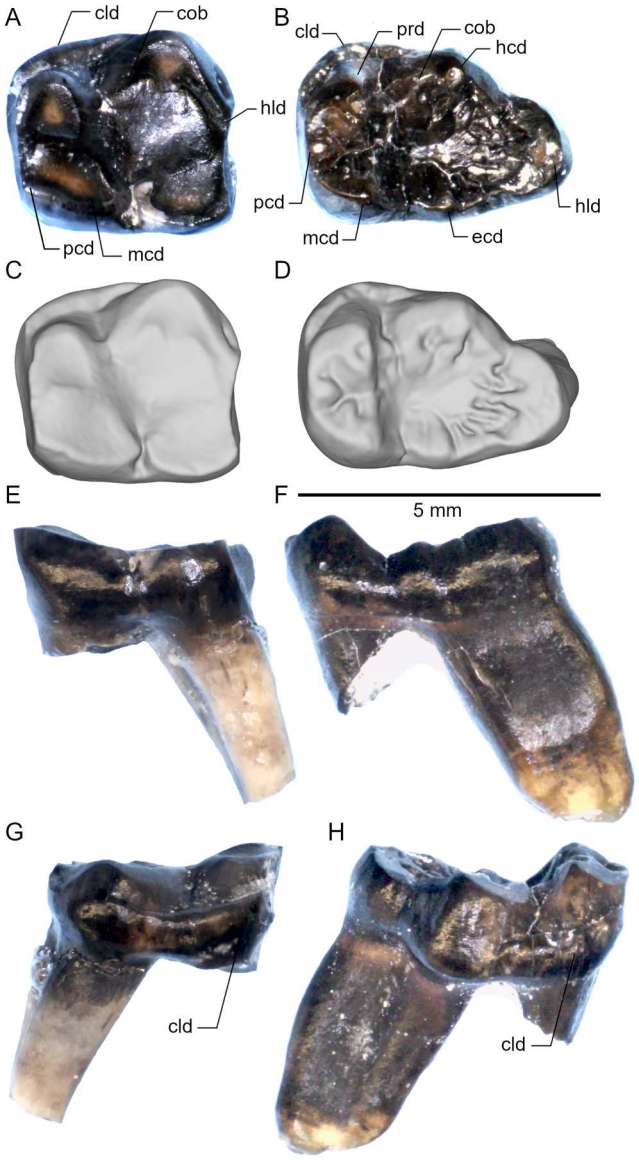

FIGURE 3. Omomyidae. Specimen FMNH PM 56655 (*Ourayia* cf. *O. uintensis*): right m2 in occlusal, **A, C** [digital 3D model], lingual, **E**, and buccal, **G** views. FMNH PM 56654 (cf. *O. uintensis*): right m3 in occlusal, **B**, **D** [digital 3D model], lingual, **F**, and buccal, **H** views. **Abbreviations**: **cld**, cingulid; **cob**, cristid obliqua; **ecd**, entoconid; **hcd**, hypoconid; **hld**, hypoconulid; **mcd**, metaconid; **pcd**, paraconid; **prd**, protoconid.

The wear pattern in the trigonid of FMNH PM 56655 seems distinctive compared with known molars of *O. uintensis* in that the paraconid and metaconid are worn down and incorporated into a single dentine pool rather than remaining separate as is usually the case. However few molars of *O. uintensis* are worn to the degree seen in this specimen, and a cursory comparison of wear patterns in previously figured specimens suggests that there is no easily definable pattern of wear exhibited by *O. uintensis*. For example, in CM 80201 (Fig. S2; Kirk et al., 2023:fig. 2m), the hypoconulid, hypoconid, cristid obliqua, protoconid, and paraconid are all worn down and incorporated into a single dentine pool, whereas the entoconid and metaconid remain separate. In CM 71069 (Fig. S2; Kirk et al., 2023:fig. 2j), the three main talonid cuspids (entoconid, hypoconid, and hypoconulid) are united in wear and separate from the trigonid cuspids. It does seem that, among trigonid cuspids, the protoconid, paracristid, and paraconid typically wear down first and form a continuous dentine pool separate from the metaconid. However, as noted above, very few specimens are worn to the degree seen in this specimen. Although not as worn, CM 71062 (Fig. S2; Kirk et al., 2023:fig. 2a) exhibits a trigonid that may have worn in a similar way based on its state of wear, the positioning of the cuspids, and the posteriorly open trigonid. This specimen also demonstrates an elongate and rounded postmetacristid, which, when worn, would give the trigonid a lingually elongated profile. The development and posterior elongation of the postmetacristid is variable in *O. uintensis*.

The development of the buccal cingulid is also variable in *O. uintensis*, with some specimens (e.g., CM 71069) exhibiting a complete buccal cingulid extending from the anterior aspect of the tooth buccal to the paraconid to the posterior aspect just buccal to the hypoconulid. At the other extreme, some specimens (e.g., CM 80201) only show development of a cingulid buccal to the cristid obliqua in between the protoconid and hypoconid, lacking a distobuccal cingulid. Most specimens fall somewhere in the middle, with a well-developed cingulid anteriorly that is discontinuous at the hypoconid. Specimen FMNH PM 56655 falls into this middle range, with a cingulid present between the protoconid and hypoconid (although it is broken anteriorly) and a weak distobuccal cingulid occurring just buccal to the hypoconulid (Fig. S2).

Although the cuspids are worn away, it is evident that the FMNH PM 56655 is more bunodont than in *H. gracilis*, including a restricted buccal cingulid and rounded cristid obliqua. Like for FMNH PM 56654, this tooth is smaller than in species of *Macrotarsius* and appears to have lacked the specialized shearing crests of that genus. Although the size and dimensions of this tooth do not preclude its assignment to *Mytonius*, the morphology of the trigonid, although worn, does not appear to have been anteroposteriorly compressed and the cuspids seem to have been more peripherally situated than in *Mytonius* (Kirk et al., 2023; Szalay, 1976).

Ourayia uintensis is known from the middle Uintan (Ui2) of the Uinta Basin, Utah and from the Washakie Formation of the Sand Wash Basin, Colorado, the age of which is unresolved (Dunn, 2024; Gazin, 1958; Gunnell et al., 2009; Kirk et al., 2023; Szalay, 1976). In addition, two specimens from the lower part of Twka2, FMNH PM 59759 (Loc. JJF 7-10-94-2) and FMNH PM 61337 (Loc. JJF 7-27-95-1), are herein tentatively referred to *O. uintensis*, pending description in a report on middle Eocene primates from the Washakie Basin; although the locality information for these specimens lacks sufficient stratigraphic resolution for secure age determinations (they may be from below or above the lowest stratigraphic datum for *Amynodon* at approximately bed 633), they indicate occurrences of *O. uintensis* in Ui1b or earlier, presuming our identification is correct. A second species, *O. coverti* Kirk, Dunn, Rodwell, and Townsend, 2023, is present in the lower Uintan (Ui1a–Ui1b) of the Tornillo Basin, Texas (Kirk et al., 2023). Additionally, two specimens are attributed to *Ourayia* sp. from the lower Uintan (Ui1b) Friars Formation of Southern California (Kirk et al., 2023). Although it is difficult to distinguish the molar teeth of *O. uintensis* from those of *O. coverti*, they consistently differ in the dimensions and morphology of the premolars, and the latter species seems to be restricted to the Tornillo Basin (for a thorough discussion, see Kirk et al., 2023). Thus, it seems more likely that the isolated teeth from Twka3 represent individuals of *O. uintensis*, as this species is well established in the central Rocky Mountain region, and no morphological features contradict assignment to this species or preferentially support assignment to *O. coverti*.

Order RODENTIA Bowdich, 1821
Family ISCHYROMYIDAE Alston, 1876
Genus *METAPARAMYS* Korth and Emry, (2007)
METAPARAMYS COMPRESSIDENS (Peterson, 1919)
(Fig. 4A)

Referred Specimens—Locality FM-4-56-WDT (~bed 677): FMNH PM 169, left dentary with i1 and p4–m3. Locality JJF 7-28-90-2 (~bed 687): FMNH PM 55361, associated left p4, m1, m2.

Comments—Wood (1962, pp. 215–217) assigned FMNH PM 169 to *Ischyrotomus compressidens*. Korth (1988) transferred *I. compressidens* to *Paramys compressidens*, but Korth and Emry (2007) later placed *P. compressidens* in the new genus *Metaparamys*. In his recent description of new fossil rodents from the Washakie Formation, Korth (2020) also referred FMNH PM 55361 to this species. These specimens share several features with *M. compressidens*, including relatively simple molars with a posteriorly open trigonid, complete ectolophid, partial hypolophid, transversely elongate hypoconulid, and lack of a mesoconid. FMNH PM 169 (Korth, 2020:fig. 1a, b) also resembles this species in having a masseteric scar extending below the anterior root of m2.

Specimen FMNH PM 55361 (Fig. 4A) was referred to "*Leptotomus*" (now *Uintaparamys* [Anderson, 2008]) *bridgerensis* by McCarroll (1995) in his meeting abstract. However, the trigonid is more distinct, the trigonid cuspids are less inflated than in *Uintaparamys*, and the ectolophids are less elongate, with less space between the metaconid and hypoconid than in the latter taxon. In these respects and in size, FMNH PM 55361 agrees well with FMNH PM 169. Accordingly, McCarroll et al. (1996a) reidentified this specimen as "*Paramys*" *compressidens*. The hypolophid in this specimen is extremely weak, consisting of a minute ridge of enamel extending buccally from the entoconid; however, its expression closely resembles USNM 20138 (Korth & Emry, 2007; Fig. 2F), which Korth and Emry (2007) refer to *M. compressidens*.

Metaparamys compressidens is otherwise known from the lower Uintan (Ui1b) Twka2 of the Washakie Formation (Korth, 2020) and the middle- and upper Uintan (Ui2–3) portions of the Uinta Formation (Korth, 1988; Gunnell et al., 2009). In a list of specimens referred to "*P.*" *compressidens* by Korth (1988), a dentary was erroneously cited as "FMNH PM 21416" (S.M.M. pers. comm. with W.W. Korth); we have not been able to locate this dentary in the FMNH collection.

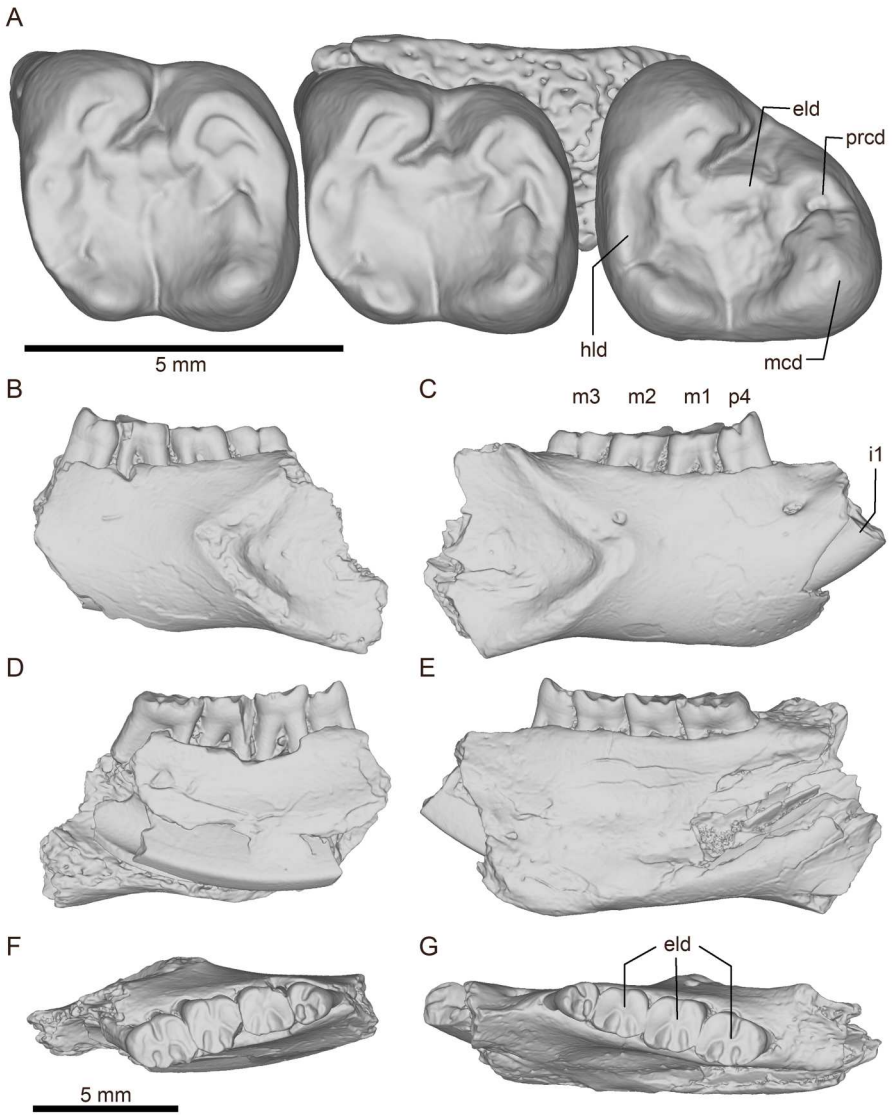

FIGURE 4. Rodentia. Specimen FMNH PM 55361 (*Metaparamys compressidens*): composite of p4, m1, and m2, **A**. Specimen FMNH PM 55060 (holotype of *Pareumys flynni*): left dentary with p4–m3 in buccal, **B**, lingual, **D**, and occlusal, **F** views; right dentary with i1, p4–m3 in buccal, **C**, lingual, **E**, and occlusal, **G** views. All images are of digital 3D models. **Abbreviations**: **eld**, ectolophid; **hld**, hypoconulid; **mcd**, metaconid; **prcd**, protoconid.

Family CYLINDRODONTIDAE Miller and Gidley, 1918
Genus *PAREUMYS* Peterson, 1919
PAREUMYS FLYNNI Korth, 2020
(Fig. 4B–G)

Holotype—Locality JJF 7-21-90-1 (~bed 677): FMNH PM 55060, right and left dentaries with i1 and p4–m3.

Comments—Specimen FMNH PM 55060 was initially identified as belonging to *Pareumys grangeri*, leading McCarroll et al. (1996a) to propose an "early Uintan" age for Twka3 (see also Walsh & Storer, 2008). Recently, Korth (2020) named and provided a thorough description of *Pareumys flynni*, designating this specimen as the holotype. *P. flynni* is similar in size to *P. grangeri* but can be distinguished from the latter species by its smaller p4 relative to molar size, p4 being approximately equal in length and width (rather than more anteroposteriorly elongate), and presence of a mesoconid on m1 in unworn specimens. It has so far only been reported from the Washakie Formation, but it is the only mammalian species in the Washakie fauna that is definitively known to be present in all levels of the Adobe Town Member (Twka1–3), albeit from a total of just six specimens (Korth, 2020). As such, the occurrence of *P. flynni* is uninformative for resolving the age of Twka3, but the ecology of this rare yet persistent species is of great interest for understanding the environmental transitions in the region from the late Bridgerian through the early/middle Uintan NALMAs.

Order HYAENODONTA sensu Solé, 2013 (amended from Van Valen, 1967)
Family HYAENODONTIDAE Leidy, 1869b
Subfamily LIMNOCYONINAE Wortman, 1902
Genus *LIMNOCYON* Marsh, 1872a
LIMNOCYON cf. *L. POTENS* Matthew, 1909
(Fig. 5)

Referred Specimen—Locality JJF 8-12-93-1 (unmeasured distance above bed 688): FMNH PM 61759, fragments of right distal humerus and right proximal radius.

Measurements—Proximodistal height of capitulum of humerus = 12.2; mediolateral width (parallel to posterior border of radial head in proximal view) × anteroposterior depth (perpendicular to the former) of head of radius = 18.9 × 12.8.

Description—The distal humerus (Fig. 5A) preserves much of the capitulum, including a capitular tail. This element is too fragmentary to provide substantial insights into the taxonomic affinities of FMNH PM 61759, but the development of the capitular tail is comparable to *Limnocyon verus* Marsh, 1872a (we examined AMNH FM 12155), consistent with identification as *Limnocyon*.

The proximal radius (Fig. 5B–D) is much more informative. The element in proximal view is ovoid, substantially wider than deep. The proximal surface is divided into three facets, a concave central facet for the capitulum, a large lateral facet articulating with the lateral capitulum and the capitular tail, and a triangular medial trochlear surface articulating with the trochlea of the humerus. Anteriorly, there is a prominent capitular eminence where the two capitular facets meet. Posteriorly, the ulnar facet is nearly flat, but there is a gentle curvature, suggesting that some capacity for pronation and supination was retained. Just distal to the head, the medial side of the radius contracts abruptly to form a well-defined neck. The surface of this constriction is rugose. Immediately distal to this constriction, on the posterior surface of the shaft, is an oval bicipital tuberosity with a central groove along its long axis.

Comments—The morphology of the proximal radius closely matches that illustrated for *Limnocyon potens* from Twka2 (Tomiya et al., 2021:fig. 18.11–13) in the shape of the radial head and the presence of an abrupt constriction medially. The only difference is the lack of a rugosity on the constricted area in *L. potens*, but this is present in at least one specimen of Bridgerian *Limnocyon verus* (FMNH UM 322). The morphology of the proximal radius of FMNH PM 61759 more generally matches Bridgerian *L. verus*, but is larger than the latter taxon, consistent with identification as *L. potens*. Compared with other hyaenodont genera known from the Uintan, *Sinopa* (e.g., *S. lania*, AMNH FM 13142) has a weaker capitular eminence and less of an abrupt transition between the radial head and neck. A proximal radius of the probable hyaenodont *Simidectes* (SDSNH 151232) lacks a transition between the head and neck entirely and has a larger, more distinct lateral facet. Postcrania are unknown in *Propterodon*, but the radius of the closely related *Hyaenodon* (e.g., AMNH FM 1381) also lacks a

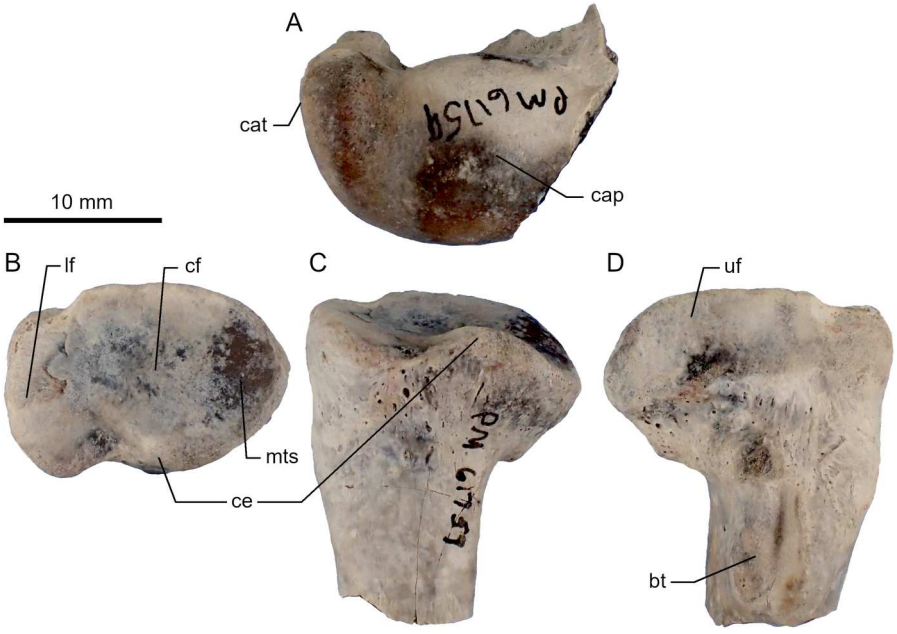

FIGURE 5. Hyaenodontidae. Specimen FMNH PM 61759 (*Limnocyon* cf. *L. potens*): right distal humerus in anterior view, **A**, and right proximal radius in proximal, **B**, anterior to bottom, anterior, **C**, and posterior, **D** views. **Abbreviations**: **bt**, bicipital tuberosity; **cap**, capitulum; **cat**, capitular tail; **ce**, capitular eminence; **cf**, capitular facet; **lf**, lateral facet; **mts**, medial trochlear surface; **uf**, proximal ulnar facet.

transition between head and neck and has a wider radial head relative to its depth.

Aside from the holotype from Twka2 and a referred specimen from the type locality, *Limnocyon potens* is represented by material from the Ui2-aged Wagonhound Member of the Uinta Formation (Peterson, 1919), including the holotype of the probable synonym *Limnocyon douglassi* Peterson, 1919. Prothero (1996) recorded *L. potens* from the Ui3-aged Myton Pocket of the Myton Member of the Uinta Formation. However, this record does not appear in other faunal lists for the Myton Member (Gunnell, 1998; Gunnell et al., 2009; Kay, 1957) and *L. potens* is not otherwise recorded after Ui2. There are records of *Limnocyon* sp. from Ui3, including a fragmentary specimen from the Hendry Ranch Member of the Wagon Bed Formation in the Wind River Basin, Wyoming (Dawson, 1980; Gazin, 1956) and more complete material from "member C" of the Santiago Formation, San Diego County, California (Walsh, 1996).

Family *Incertae Sedis*
Genus *SIMIDECTES* Stock, 1933
SIMIDECTES sp.
(Fig. 6)

Referred Specimen—Locality JJF 7-28-90-2 (~bed 687): FMNH PM 55362, left astragalus.

Measurements—Greatest proximodistal length of astragalus (perpendicular to distal margin of astragalar head, measured in anterior view) = 28.3; greatest mediolateral width of astragalus (perpendicular to length) = 22.7.

Description—Specimen FMNH PM 55362 is a left astragalus missing the proximoventral margin due to specimen erosion/breakage, including the proximomedial plantar tuberosity and the groove for m. flexor digitorum lateralis. The lateral tibial facet is distinctly grooved, with the groove placed closer to the medial margin of the facet. The lateral portion of the lateral tibial facet is taller than the medial portion in distal view. The lateral tibial facet is sharply offset from the medial tibial facet. The distal margin of the lateral tibial facet is concave, forming a pit for reception of the distal tibia. Medial to the distal half of the tibial facet is a distinct cotylar fossa. The lateral surface of the astragalar body is formed by a crescentic, laterally oriented fibular facet. Proximally, an astragalar foramen is present. The foramen is hidden in dorsal view by the lateral tibial facet. On the ventral surface of the astragalar body, the preserved portion of the ectal facet is transversely narrow and inclined distolaterally, overhanging the remainder of the body distally to support a prominent lateral process in dorsal view.

The astragalar neck is well-defined and inclined distomedially such that the head only partially overlaps the body. On the ventral surface of the neck, the sustentacular facet is large, circular, and does not contact the ventral margin of the neck. The head is dominated by the navicular facet (likely including a contact surface with the cuboid as well). The long axis of the facet is oblique, and the facet is flat transversely, but curved dorsoplantad. Medially, the facet extends up the medioplantar margin of the neck to overlap the sustentacular facet. On the lateroplantar margin of the head is a prominent distal sustentacular facet.

Comments—Specimen FMNH PM 55362 is identified as *Simidectes* based on comparisons to an associated partial skeleton of *S. medius* (Peterson, 1919) from "member C" (see Walsh [1996] on stratigraphy) of the Santiago Formation, San Diego County, California (SDSNH 32182). Significant points of resemblance include: deeply grooved trochlea; pit for reception of the distal tibia; narrow, oblique ectal facet; cotylar fossa on the distal half of the medial tibial facet; long axis of the navicular facet oriented more parasagittally than transversely; and large distal sustentacular facet.

Simidectes is known from Ui2 through Duchesnean-aged deposits of western North America, including in Utah, Texas, and southern California (Coombs, 1971; Golz & Lillegraven, 1977; Gunnell et al., 2009; Gustafson, 1979; Stock, 1933; Walsh, 1996; Westgate, 1990; Wilson & Stevens, 1986); an earlier record from the Ui1b-aged Friars Formation of southern California has been reported, but not yet described (Zack, 2023). In addition, a possible relative of *Simidectes* has been reported from Twka1 based on a single lower molar, but its generic attribution is uncertain (Tomiya et al., 2021).

unranked clade CARNIVORAMORPHA sensu Bryant, 1996 (amended from Wyss and Flynn [1993]; see also Pan-Carnivora of Flynn et al. [2020])
unranked clade CARNIVORAFORMES Flynn, Finarelli, and Spaulding, 2010
CARNIVORAFORMES gen. et sp. indet.
(Fig. 7)

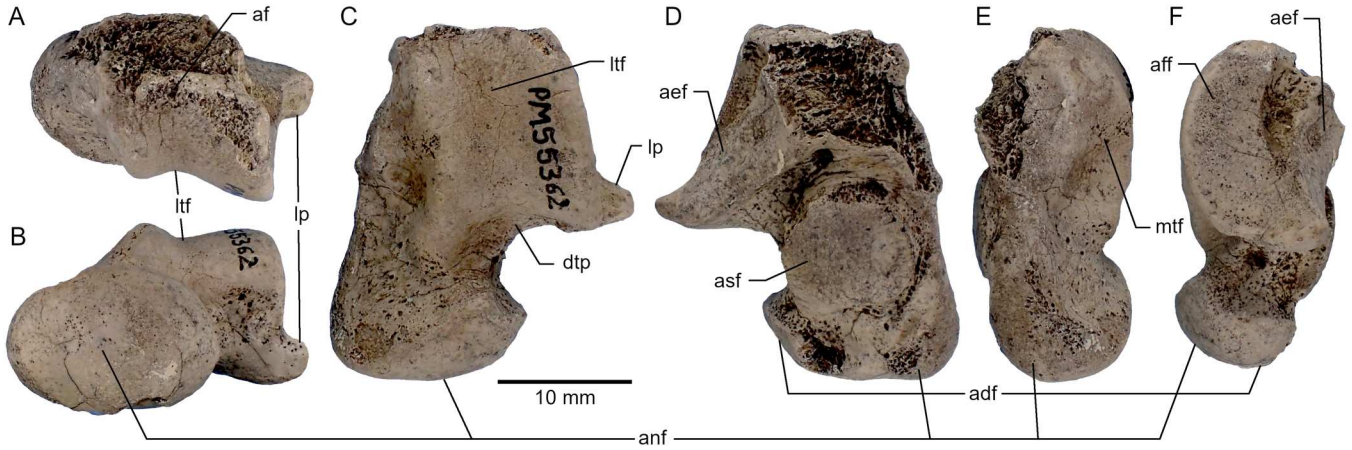

FIGURE 6. *Simidectes* sp. Specimen FMNH PM 55362: left astragalus in proximal, **A**, distal, **B**, dorsal, **C**, medial, **D**, and lateral, **E** views. **Abbreviations**: **adf**, astragalar distal sustentacular facet; **aef**, astragalar ectal facet; **af**, astragalar foramen; **aff**, astragalar fibular facet; **anf**, astragalar navicular facet; **asf**, astragalar sustentacular facet; **dtp**, distal tibial pit; **lp**, lateral process; **ltf**, lateral astragalar tibial facet; **mtf**, medial astragalar tibial facet.

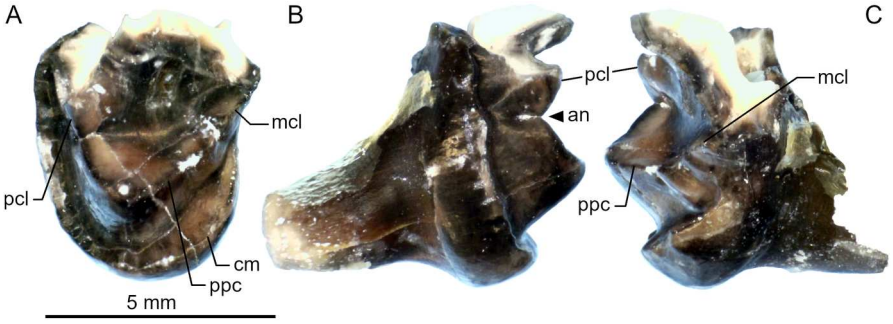

FIGURE 7. Carnivoraformes. Specimen FMNH PM 56222 (Carnivoraformes gen. et sp. indet.): partial left M1 in occlusal, **A,** anterior, **B**, and posterior, **C** views. **Abbreviations**: **an**, anterior notch; **cm**, cingulum; **mcl**, metaconule; **pcl**, paraconule; **ppc**, postprotocrista.

Referred Specimen—Locality JJF 8-12-93-2 (~bed 687): FMNH PM 56222, partial left M1.

Description—Specimen FMNH PM 56222 is the lingual half of a left M1 with minimal wear. The tooth has a heavy cingulum that terminates along the posterior border of the tooth. The cingulum maintains a roughly constant width along the anterior border of the crown, but broadens posterolingually, such that its broadest portion is roughly twice as thick as the anterior portion. The posterolingual portion of the cingulum creates a deep valley, rather than a level shelf, between its sharp posterior edge and the trigon, without forming a distinct posterolingual cusp. The enamel layer shows fine (anteriorly) to coarse (posterolingually) crenulation along the margin of the cingulum. The protocone is anteroposteriorly asymmetrical, with its apex located anteriad but not so much as to interrupt the lingual cingulum. There is a prominent notch associated with a small incision at the anterobuccal terminus of the preprotocrista. The buccal segment of this notch pertains to a weakly developed paraconule whose buccal portion is not preserved. The postprotocrista bears two shallow incisions. The slightly raised segment between them could be interpreted as either an incipient or vestigial protoconule. Immediately posterior to this structure, a poorly developed metaconule is present, which bears a slightly raised ridge that continues from the postprotocrista. The paracone and metacone are broken off and largely missing.

Measurements—L × W of preserved portion = 5.0 × 5.8.

Comments—Specimen FMNH PM 56222 was previously reported as "*Miacis* sp." in the faunal table of McCarroll et al. (1996a). Given that the genus *Miacis* as currently recognized is likely polyphyletic and lacks an apomorphy-based diagnosis (Solé et al., 2016; Spaulding & Flynn, 2012; Tomiya et al., 2021), we instead conservatively assign this specimen only to Carnivoraformes, based on the continuous lingual cingulum of M1 along the base of the protocone—a trait that is absent in viverravid carnivoramorphans (Tomiya et al., 2021). In comparison to known Uintan carnivoraforms, it differs from the M1s of: *Tapocyon* Stock, 1934, *Miocyon* Matthew, 1909, and *Ceruttia* Tomiya, 2013, in the greater development and more pronounced anteroposterior asymmetry of the lingual cingulum (cf. Dawson, 1980; Wesley & Flynn, 2003; Tomiya, 2013); *Procynodictis* Wortman and Matthew, 1899, and *Walshius* Tomiya, 2013, in the continuity of the lingual cingulum along the base of the protocone (Tomiya, 2013); and '*Miacis*' *gracilis* Clark, 1939, and likely '*M.*' *hookwayi* Stock, 1934, in having a relatively longer protocone with a more posteriorly oriented postprotocrista (cf. Tomiya, 2013). Specimen FMNH PM 56222 compares well with *Lycarion medius* (Matthew, 1909), '*Miacis*' *invictus* Matthew and Granger, 1925, *Neovulpavus washakius* Wortman, 1901, and *N. mccarrolli* Tomiya, Zack, Spaulding, and Flynn, 2021, in its well-developed lingual cingulum and the forms and configuration of the protocone, paraconule, and metaconule. Although the specimen from Twka3 is too incomplete to establish its conspecificity with any of these four species, they all are known from the middle Eocene (*L. medius*, *N. washakius*, and *N. mccarrolli* occur in Twka1 or Twka2 of the Washakie Formation) and are likely close relatives that are collectively more closely related to the crown carnivorans than to early-Eocene carnivoraforms (Tomiya et al., 2021). There are no well-preserved M1s of '*Miacis*' *uintensis* Osborn, 1895, known from the Uinta Formation (Matthew, 1909; Spaulding and Flynn, 2009), precluding comparison with that taxon. Likewise, the upper dentition of *Uintacyon acutus* Thorpe, 1923, is not known, but FMNH PM 56222 differs generally from M1s of the genus *Uintacyon* Leidy, 1873, in the greater development and more pronounced anteroposterior asymmetry of the lingual cingulum.

Order ARTIODACTYLA Owen, 1848
Family HOMACODONTIDAE Marsh, 1894
Genus *MESOMERYX* Peterson, 1919
MESOMERYX cf. *M. GRANGERI* Peterson, 1919
(Fig. 8)

Referred Specimen—Locality JJF 8-12-93-2 (~bed 687): FMNH PM 56652, partial left M1.

Measurements—Posterior W across metacone and metaconule = 4.7.

Description—Specimen FMNH PM 56652 lacks the anterobuccal portion of the crown, such that the morphology of the parastyle and paracone cannot be determined. A lingual portion of a small paraconule is preserved, and the preparaconule-crista, which lingually connects to the preprotocrista, shows moderate wear (Fig. 8A, D). The protocone and metaconule are subequal in size. The former has a well-defined preprotocrista and only a very faint postprotocrista. The weakness of the postprotocrista, combined with better developed crests on the metacone and metaconule, confers a bunoselenodont appearance to the crown. Although most of the anterior border of the tooth is missing, a small part of the anterior cingulum is present near the base of the protocone. The metaconule bears well developed pre- and post-metaconule-cristae, contributing to a somewhat crescentic outline of the buccal face of this cuspule. On the metacone, moderately sharp pre- and post-metacristae mark the borders of the weakly convex buccal facet of the cusp, which shows weak ribbing. The premetacrista and the anterobuccal base of the metacone are sufficiently preserved to suggest that a mesostyle was either absent or small at most. A posterolingual cingulum stretches from the posterolingual base of the protocone to the posterior base of the metaconule. Although the enamel surface of this cingulum is coarsely crenulated between the bases of the protocone and metaconule, it does not form a recognizable hypocone.

Comments—Specimen FMNH PM 56652 is likely the basis for the occurrence of "cf. *Mesomeryx grangeri*" in Twka3 reported by

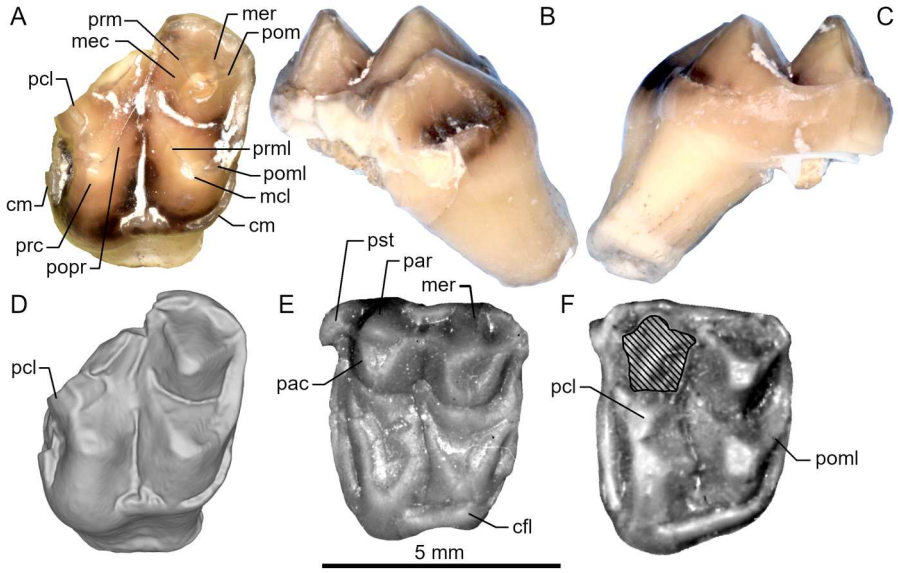

FIGURE 8. Homacodontidae. Specimen FMNH PM 56652 (*Mesomeryx* cf. *M. grangeri*): partial left M1in occlusal, **A**, **D** [digital 3D model], anterior, **B**, and posterior, **C** views. Cast of holotype CM 3189 from Uinta Formation: left M1 in occlusal view, **E** (rest of tooth row not shown). Specimen FMNH 59826 (*M. grangeri*; original specimen from Uinta Formation): left M1 in occlusal view, **F** (rest of tooth row not shown). **Abbreviations**: **cfl**, flexure of cingulum; **cm**, cingulum; **mcl**, metaconule; **mec**, metacone; **mer**, metacone rib; **pac**, paracone; **par**, paracone rib; **pcl**, paraconule; **pom**, postmetacrista; **poml**, postmetaconule-crista; **popr**, postprotocrista; **prc**, protocone, **prm**, premetacrista; **prml**, premetaconule-crista; **pst**, parastyle.

Covey and McCarroll (1996) and McCarroll et al. (1996a:table 1). We refer this specimen to the monotypic genus *Mesomeryx* based on its very small size, the moderate degree of selenodonty (as perceived from the convexity of the metacone and the sharpness of major crests), and the lack of a hypocone (cf. Theodor et al., 2007). In these respects, the specimen closely resembles M1s of the holotype of *M. grangeri*, CM 3189 (we examined its cast, as the original specimen was missing from the CM collection; Fig. 8E), from the Uinta B or C horizon (cf. Gazin, 1955) and FMNH PM 59826 (cast of a missing and, at the time of casting, uncatalogued specimen, originally in D.T. Rasmussen's collection at Washington University in St. Louis; Fig. 8F) from the Ui2-aged portion of the Uinta Formation, Utah (cf. Townsend et al., 2006). In addition, both FMNH PM 56652 and FMNH PM 59826 have a distinct, if small, paraconule, as conjectured by Gazin (1955) for the heavily worn holotype CM 3189 (note that Peterson [1919:73] and Gazin [1955:30] referred to the paraconule in the present usage as "protoconule"), but in conflict with its characterization as "barely apparent" (Stucky, 1998:368) or absent (Theodor et al., 2007) in *M. grangeri*. The "flexure," or subtle bulging, of the posterolingual cingulum lingual to the base of the metaconule on M1 reported by Gazin (1955) for the holotype ("cfl" in Fig. 8E), and repeated by Stucky (1998) and Theodor et al. (2007), is absent in the M1s of FMNH PM 56652 and FMNH PM 59826, raising a question about its taxonomic significance. The buccal ribbing of the metacone appears somewhat weaker in FMNH PM 56652 than in FMNH PM 59826 and CM 3189. These minor variations among otherwise closely-resembling specimens and the incompleteness of the material from Twka3 prevent us from definitive species-level identification of FMNH PM 56652, and we await detailed descriptions of thus-far unpublished dental specimens from the Uinta Formation (cf. Rasmussen et al., 1999; Townsend et al., 2006). FMNH PM 56652 is identified as an M1 rather than an M2 because the latter tooth is substantially larger in *M. grangeri* (cf. Gazin, 1955) and has a buccolingually narrower metaconule relative to the protocone.

At present, *Mesomeryx grangeri* is generally considered an index species of biochron Ui2 (cf. Gazin, 1955; Gunnell et al., 2009; Townsend et al., 2006). However, we have identified in the FMNH collection dental specimens from Twka2 that are referable to *M. grangeri*, which suggests occurrence of the species also in the early Uintan (Ui1b) interval (cf. Gunnell et al., 2009; Tomiya et al., 2021); we intend to describe these specimens in a forthcoming paper on artiodactyl fossils from Twka1 and Twka2.

ARTIODACTYLA gen. et sp. indet.
(Fig. 9)

Referred Specimen—Locality JJF 8-12-93-2 (~bed 687): FMNH PM 61240, right astragalus.

Measurements—Greatest proximodistal length of astragalus (perpendicular to distal border of distal trochlea) = 16.3; distal width of proximal trochlea of astragalus = 9.9; width of distal trochlea of astragalus (measured in distal view) = 8.7.

Description—The grooves of the proximal and distal trochleae are approximately aligned, but the former is ~50% deeper along the dorsoplantar axis than the latter (Fig. 8A, B). The two trochleae are separated by a moderately long neck, whose long axis is tilted in the proximolateral to distomedial direction. The proximal trochlea is marked by its asymmetry, owing to the dorsomedially facing facet (bearing the lateral trochlear ridge) that is roughly three times as wide as the dorsolaterally facing facet (bearing the medial trochlear ridge). The ectal facet is a narrow strip whose proximal portion faces distolaterally, being part of a lateral protrusion (not homologous with the lateral process in non-artiodactyl mammals; cf. Geisler, 2001), and its distal portion is more laterally oriented. The laterally positioned sustentacular facet has an elliptical outline in plantar view, and forms a convex surface in lateral view. In dorsal view, the distal trochlea is clearly divided by a ridge into the cuboid facet, which occupies roughly the lateral one-quarter of the width of the trochlea, and the navicular facet. The trochlear groove is positioned near the midline of the navicular facet.

Comments—We have compared FMNH PM 61240 with astragali of small artiodactyls from Twka1 and Twka2 (including multiple homacodontid taxa and possibly a helohyid) that are in the FMNH collection, and also with images of other comparably-sized middle Eocene artiodactyls of North America (e.g., oromerycids, protoceratids). However, we have not been able to determine the affinity of the specimen from Twka3 below the ordinal rank of Artiodactyla. The combination of a relatively long neck and a wide and strongly asymmetric proximal trochlea, which characterizes FMNH PM 61240, is also seen in FMNH PM

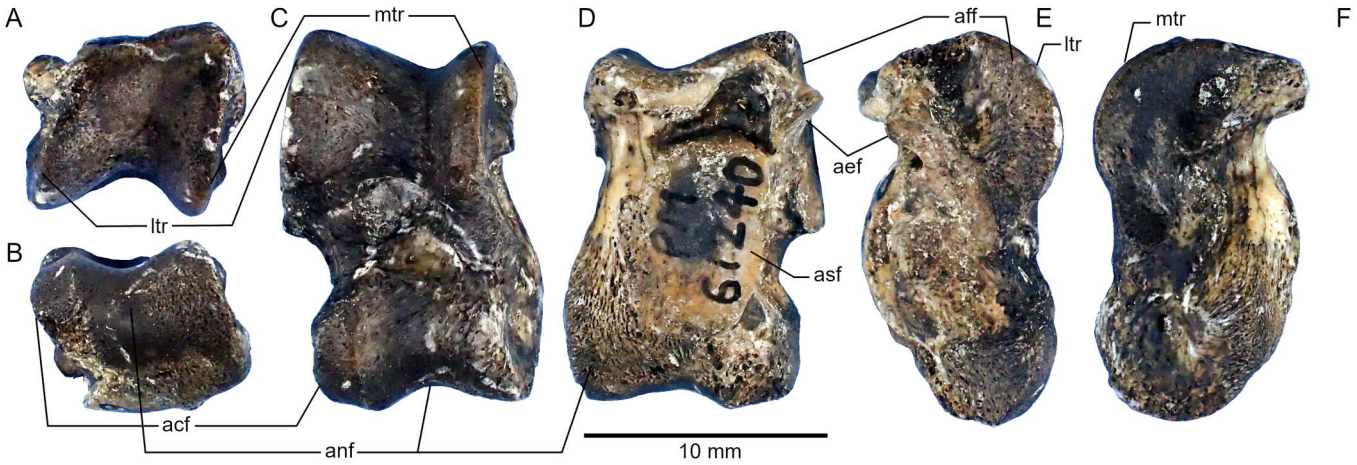

FIGURE 9. Other artiodactyls. Specimen FMNH PM 61240 (Artiodactyla gen. et sp. indet.): right astragalus in proximal, **A**, distal, **B**, dorsal, **C**, plantar, **D**, lateral, **E**, and medial, **F** views. **Abbreviations**: **acf**, astragalar cuboid facet; **aef**, astragalar ectal facet; **aff**, astragalar fibular facet; **anf**, astragalar navicular facet; **asf**, astragalar sustentacular facet; **ltr**, lateral trochlear ridge; **mtr**, medial trochlear ridge.

61400 from Twka1, raising the possibility that the lineage to which FMNH PM 61240 belongs was present in the region in the late Bridgerian (Br3). Unfortunately, neither of these astragali is accompanied by taxonomically diagnostic dental material. FMNH PM 61240 is roughly 60% longer in its proximodistal dimension than the diminutive astragalus of *Mesomeryx grangeri* from the Uinta Basin illustrated by Rasmussen et al. (1999: fig. 10). The former yields an estimated body mass of ~6 kg using Martinez and Sudre's (1995) allometric equation based on extant non-cetacean artiodactyl data. Thus, it evidently belongs to a taxon that is considerably larger than that represented by FMNH PM 56652 (*Mesomeryx* cf. *M. grangeri*), described above, and indicates the presence of at least two disparately sized artiodactyl taxa in Twka3.

Order PERISSODACTYLA Owen, 1848
Suborder HIPPOMORPHA Wood, 1937
Family EQUIDAE Gray, 1821
Genus *EPIHIPPUS* Marsh, 1878
EPIHIPPUS GRACILIS (Marsh 1871)
(Fig. 10, S3)

Referred Specimen—Locality JJF 7-21-90-1 (~bed 677): FMNH PM 55311, crown of left dp2, partial left dentary with roots of p1, roots of dp2, dp3, dp4, m1–m2, and unerupted partial m3, and associated tooth fragment.

Measurements—dp2L = >5.5 (missing paraconid); dp2 trigonid W = 2.9; dp2 talonid W = 3.3. See McCarroll et al. (1996b) for measurements of dp3–m2.

Description—Specimen FMNH PM 55311 was figured and described by McCarroll et al. (1996b), and discussed by Rose et al. (2018). Although not mentioned in the original description, the paraconid of the left dp2 is broken off, and so its morphology is unknown (Fig. 10D). We confirm that the "postcristid branch" of the dp2, as referred to in McCarroll et al. (1996b), is the same structure as the hypoconulid crest of Rose et al. (2018), and that its position and extent in FMNH PM 55311 are similar to those in the holotype YPM VP 011271 of *Epihippus gracilis* (Granger, 1908:pl. 18, fig. 4) and AMNH FM 2042 from the Uinta Formation (referred to *E. gracilis* by Granger [1908] and described in detail by Rose et al. [2018:fig. 15]). The metaconid of the dp3 is located lingually (Fig. 10D), as noted by Rose et al. (2018) for AMNH FM 2042, and not "at the midline of the tooth", as initially reported by McCarroll et al. (1996b:6). On the dp3, no lingual cingulid is discernible (contra McCarroll et al., 1996b), while a buccal cingulid is present anterobuccal to the hypoconid, in agreement with Rose et al.'s (2018) observation of AMNH FM 2042.

Comments—The morphology, including the degree of dilambdodonty of dp3–dp4, and sizes of dp2–dp4 in FMNH PM 55311 are closely comparable to those in YPM VP 011271 and AMNH FM 2042. The single-rooted p1 (Fig. 10B, C) distinguishes *Epihippus* from *Orohippus* Marsh, 1872b, and *Haplohippus* McGrew, 1953, the two other equid genera that are known from the middle Eocene of North America (MacFadden, 1976). In addition, the rounded anterobuccal bend of the m2 paralophid (Fig. 10C) is consistent with *Epihippus* and not *Orohippus* (cf. Froehlich, 2002).

The known temporal range of *Epihippus gracilis* is Ui1a (Murphey & Kelly, 2017) to Ui3 (Gunnell et al., 2009). Despite their occurrence throughout the Uintan NALMA, this species and, more generally, the genus *Epihippus* are thus far unknown from the Ui1b portion of Twka2. Although the Bridgerian equid *Orohippus* is known from several specimens (including those reported by McCarroll et al., 1996b) from Twka1, the rarity of equid fossils in the Washakie Formation conforms to the general pattern in the middle Eocene of North America noted by MacFadden (1998).

Suborder TAPIROMORPHA Haeckel, 1866
Infraorder CERATOMORPHA sensu Hooker, 2005
(amended from Wood, 1937)
Family AMYNODONTIDAE Scott and Osborn, 1883
Genus *AMYNODON* Marsh, 1877
AMYNODON ADVENUS (Marsh, 1875)
(Fig. 11)

Referred Specimens—Locality FM-8-69-WDT (bed ~680–687): FMNH PM 61725, fragmentary teeth including right P3 or P4 and right M2 or (less likely) M1; FMNH PM 61739, fragmentary teeth including canine (right c1?), right p3, right m3, left m2.

Measurements—Specimen FMNH PM 61725: RM2 (or M1) ectoloph L (measured parallel to its long axis) = 47.6. FMNH PM 61739: Rp3L × W = 18.5 × 13.3; L of preserved portion of Lm2 = 38.0; L of preserved portion of Rm3 = 40.5.

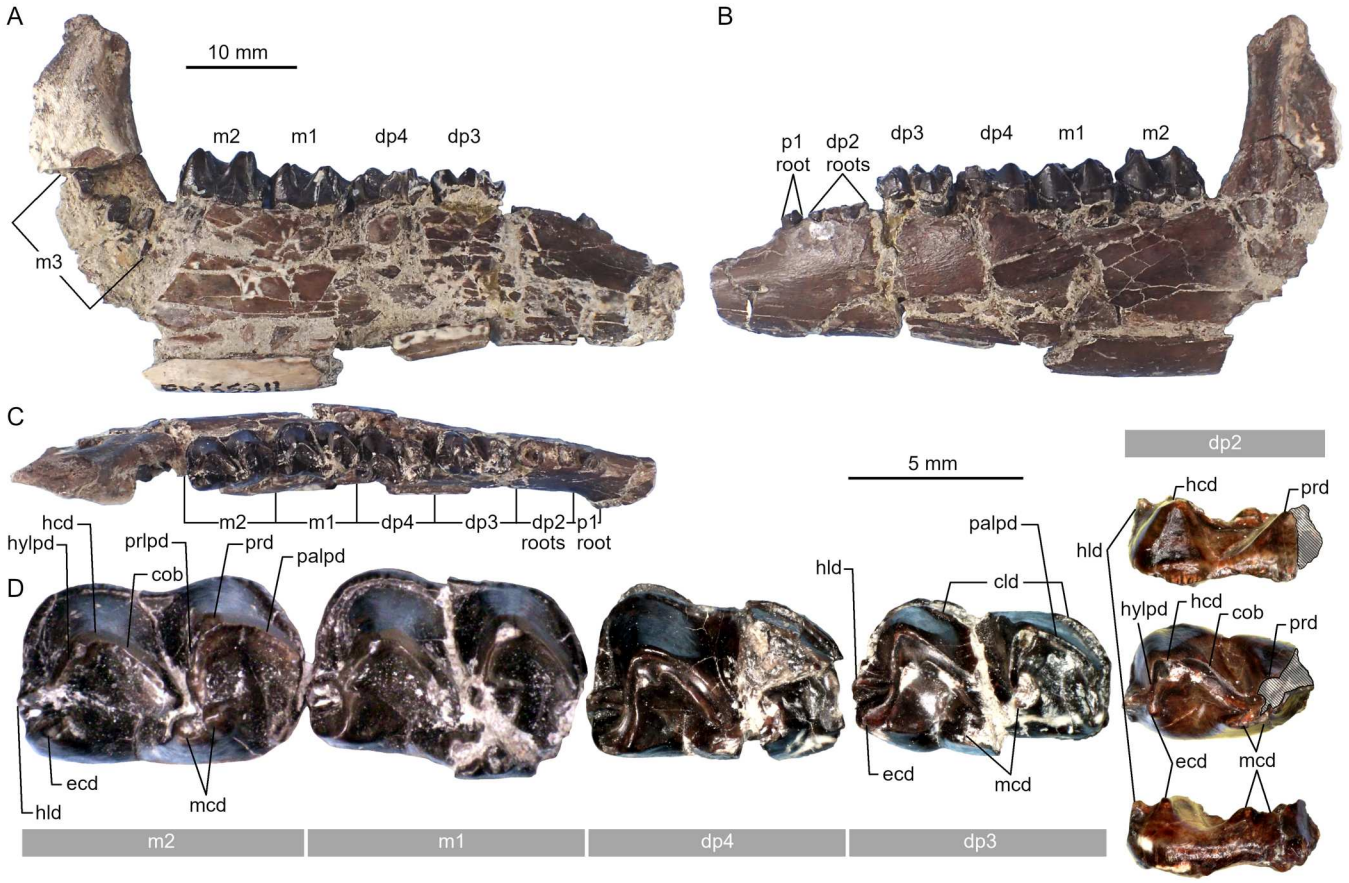

FIGURE 10. Equidae. Specimen FMNH PM 55311 (*Epihippus gracilis*): left dentary in medial, **A**, lateral, **B**, and occlusal, **C**; composite of left dp2 (in buccal [reversed], occlusal, and lingual views, respectively, from top to bottom)—m2, **D**. Different scale bars apply to **A**–**C** and **D**. **Abbreviations**: **cld**, cingulid; **cob**, cristid obliqua; **ecd**, entoconid; **hcd**, hypoconid; **hld**, hypoconulid; **hylpd**, hypolophid; **mcd**, metaconid; **palpd**, paralophid; **prd**, protoconid; **prlpd**, protolophid.

Description—The crown of a right p3 belonging to FMNH PM 61739 is completely preserved and shows little wear (Fig. 11C–E). Its dimensions are well within the ranges of p3 measurements reported by Wall (1982:table 1) for a total of 18–19 specimens of *A. advenus* from Texas and the central Rocky Mountain region. This tooth shows a lesser degree of molarization than the p4, and is dominated by the tall protoconid. Other cuspids are not clearly recognizable, but the sharp ridges that descend from the apex of

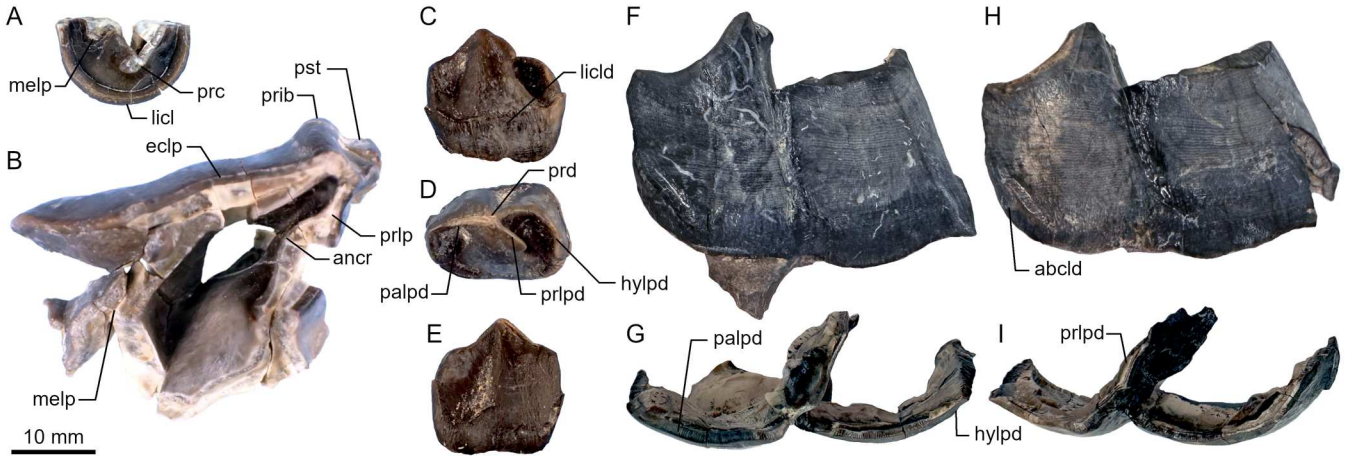

FIGURE 11. Amynodontidae. Specimen FMNH PM 61725 (*A. advenus*): partial right P3 or P4 in occlusal view, **A**; partial right M2 or (less likely) M1 in occlusal view, **B**. FMNH PM 61739 (*A. advenus*): right p3 in lingual, **C**, occlusal, **D**, and buccal, **E** views; partial left m2 in buccal, **F** and occlusal, **G** views and partial right m3 (reversed) in buccal, **H** and occlusal, **I** views. **Abbreviations**: **abcld**, anterobuccal cingulid; **ancr**, antecrochet; **eclp**, ectoloph; **hylpd**, hypolophid; **licl**, lingual cingulum; **licld**, lingual cingulid; **melp**, metaloph; **palpd**, paralophid; **prc**, protocone; **prd**, protoconid; **prib**, paracone rib; **prlp**, protoloph; **prlpd**, protolophid; **pst**, parastyle. Different scale bars apply to **A**–**G** and **H**–**M**.

the protoconid along its anterior, lingual, and posterior slopes may be interpreted as, respectively, a paralophid, a protolophid, and a cristid obliqua followed by a lingually directed hypolophid. The base of the crown is surrounded by a well developed cingulid that is particularly deep on the lingual side. Although the rest of FMNH PM 61739 is highly fragmentary, elements of this specimen preserve enough characters to be identified as *Amynodon advenus*. For example, the partial lower molars of FMNH PM 61739 exhibit: (1) posterolingual orientations of the protolophids and hypolophids (Fig. 11G, I); and (2) a distinct groove separating the trigonid from the talonid that are diagnostic of the genus *Amynodon* (Fig. 11F, H). The relatively large sizes of the teeth are consistent with *A. advenus* rather than *A. reedi* (Wall, 1982). In addition, the following characters are noticed from the fragmentary teeth: the trigonid has roughly equal height and length with those of talonid; a distinct anterobuccal cingulid is discernible.

The referral of FMNH PM 61725 to *Amynodon advenus* is more provisional given the limited suite of upper dental characters that are considered diagnostic of the genus *Amynodon* or *A. advenus* (cf. Wall, 1982), but in their forms and sizes, the upper teeth closely resemble those of other specimens of *A. advenus* from elsewhere. The partial upper premolar, representing a P3 or P4 (Fig. 11A), bears a thick lingual cingulum that is continuous along the entire rim of the preserved portion, and a protoloph and a metaloph that do not converge lingually. These traits are also seen in FMNH PM 1088 from Twka2 (McCarroll et al., 1996b), but they are apparently variable within *A. advenus* (Wall, 1982; Wilson & Schiebout, 1981). The moderately worn upper molar is dominated by the long and nearly straight ectoloph (Fig. 11B). Distinct parastyle and anterior ectoloph rib are present, while no posterior ectoloph rib is recognizable (contra Wall [1982:439] but consistent with Wilson and Schiebout's [1981:16] description). Both the protoloph and metaloph are slanted posteriad in occlusal view. The weak development of antecrochet on the protoloph suggests that this tooth is more likely an M2 than an M1 (cf. Wilson & Schiebout, 1981; Wall, 1982). Lack of buccal deflection of the metastylar region precludes this tooth from being an M3 (cf. Wall, 1982).

Comments—*Amynodon advenus* was previously reported from Twka2 (McCarroll et al., 1996b). There are no definitive records of its occurrence below Roehler's (1973) bed 633, and so a significant lower portion of Twka2 may pre-date biochron Ui1b (cf. McCarroll et al., 1996a; Murphey et al., 2018; Tomiya et al., 2021). The referred specimens here extend this species' stratigraphic range within the Washakie Formation upwards to include at least part of the upper unit of the Adobe Town Member. In North America, *A. advenus* is known from biochrons Ui1b through Ui3 of the Uintan NALMA (Gunnell et al., 2009).

AMYNODON cf. *A. ADVENUS*
(Fig. 12A–C)

Referred Specimen—Locality JJF 8-12-93-2 (~bed 687): FMNH PM 56656, left p2.

Measurements—L (preserved portion) = 12.3; W (preserved portion) = 9.4.

Description—The crown of FMNH PM 56656 is missing the tip of the protoconid and the posterior to posterobuccal surface (Fig. 12A, B). It is dominated by a centrally located protoconid. The anterior slope of the protoconid bears a well-developed ridge (= "paralophid" of Wall [1982:44]) that swings lingually to merge with the deep lingual cingulid (Fig. 12A, C). Another ridge (= "protolophid" of Wall [1982:44]) descends from the apex of protoconid along the posterolingual surface of the crown and swings lingually toward its base to intersect the lingual cingulid; this posterolingual ridge marks the anterior border of a somewhat concave posterolingual facet (= "talonid" of [Wall 1982:44]). Although the posterior margin of the crown is not preserved, the curvature of the posterolingual portion of the crown indicates that the concave posterolingual facet was short (Fig. 12A). A thin anterobuccal cingulid is also present (Fig. 12A, B). This tooth is single-rooted (Fig. 12B, C).

Comments—Wall (1982) considered presence of large and double-rooted p2 to be one of the diagnostic traits of the genus *Amynodon*. However, CM 3434 and AMNH FM 1963, both mandibular specimens of *A. advenus* from the Uinta Formation of Utah, preserve p2s with at least partially fused anterior and posterior roots, as indicated by a shallow longitudinal groove on the lingual side (Fig. 12F). The p2 of CM 3434 in particular is closely comparable to that of FMNH PM 56656 in size (L = 13.6, W = 9.2) and in all the morphological traits described above (Fig. 12D–F). The dimensions of p2s in these two specimens, in turn, are near the upper limits of previously reported ranges of measurements (L = 10–13, W = 7–10) for 7 specimens of *A. advenus* from Utah and Wyoming, but it should be noted that the p2 is the most variable among the lower cheek teeth of *Amynodon* in terms of anteroposterior length (Wall, 1982:table 1). The referral of CM 3434 to *A. advenus* rather than the distinctly smaller *A. reedi* is justified on the basis of its molar row lengths (Lm1–m3L = ~96, with heavy wear), which fall near the mean value for *A. advenus* (Wall, 1982). Because the number of roots is often difficult to ascertain based on external observation when the tooth is in place, we suspect that occurrences of p2s with a single root (as in FMNH PM 56656) or a fused pair of roots (as in CM 3434) have gone unnoticed in *Amynodon*, and that such variation can be accommodated within a species, especially in a lineage that subsequently underwent reduction and loss of this tooth (cf. Wall, 1982).

CERATOMORPHA gen. et sp. indet.
(Fig. 13)

Referred Specimen—Locality JJF 8-12-93-2 (~bed 687): FMNH PM 62461, partial left astragalus.

Description—The astragalus is missing the lateral portions of the trochlea, neck, and head, as well as a proximoplantar portion of the medial half. Judging from the preserved portion, the astragalus appears to have been proximodistally somewhat longer than mediolaterally wide (Fig. 13B). The neck is very short, such that the distal extremity of the medial trochlear ridge is almost in contact with the dorsomedial corner of the navicular facet. Similar conditions have been noted or illustrated for the tapiroid *Hesperaletes borineyi* from the upper Uintan of California (Colbert, 2006a), and the ceratomorphs *Lophialetes expeditus* and *Deperetella cristata* from the upper middle Eocene of northeast Asia (Radinsky, 1965:figs. 30, 39). In dorsal view, the medial trochlear ridge of FMNH PM 62461 is oriented at an angle of ~15° from the proximodistal axis of the astragalus (here defined perpendicular to the distal border of the astragalar head). This degree of trochlear inclination is similar to that in *L. expeditus* (~15°; Radinsky, 1965) and appreciably less than in *H. borineyi* (~20–25°; Colbert, 2006a). The navicular facet is saddle-shaped, as is diagnostic of Perissodactyla (Radinsky, 1966), showing a moderate convexity and a weak concavity along the dorsoplantar and mediolateral axes, respectively. The cuboid facet is apparently not preserved. On the plantar side, the laterally positioned sustentacular facet is proximodistally extensive and bends laterad toward its distal end. Its preserved portion forms a mostly flat surface.

Comments—Although the breakages precluded standard measurements from being taken on FMNH PM 62461, the preserved portion suggests original dimensions that were roughly

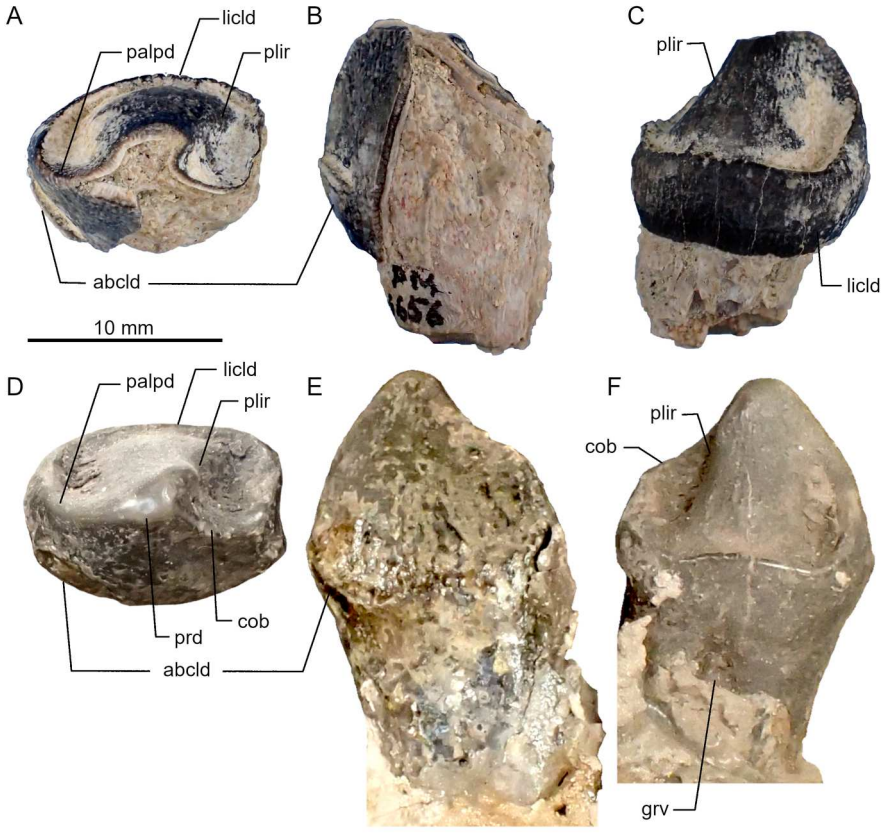

FIGURE 12. Amynodontidae (continued). Specimen FMNH PM 56656 (*Amynodon* cf. *A. advenus* from Twka3): left p2 in occlusal, **A**, buccal, **B**, and lingual, **C** views. CM 3434 (*A. advenus* from Uinta B horizon): left p2 (rest of tooth row not shown) in occlusal, **D**, buccal, **E**, and lingual, **F** views. **Abbreviations**: **abcld**, anterobuccal cingulid; **grv**, groove between fused anterior and posterior roots; **licld**, lingual cingulid; **cob**, cristid obliqua; **palpd**, paralophid; **plir**, posterolingual ridge; **prd**, protoconid.

comparable to those of *Hesperaletes borineyi* (cf. Colbert, 2006a), for which Tomiya (2012) estimated a body mass of ~11 kg based on M1 measurements reported by Colbert (2006b). The notably short neck and the relatively shallow slope of the medial condyle of the trochlear facet (i.e., a less acute medial trochlear ridge) distinguish this astragalus from those of early equids, chalicotheriids, and isectolophids (cf. Osborn, 1913; Froehlich, 1999; Maas et al., 2001). We conservatively refer this specimen to Ceratomorpha, given the incompleteness of the material and unresolved phylogenetic systematic issues surrounding early ceratomorphs (Hooker, 2005; Bai et al., 2020). The astragalar forms of small ceratomorphs that occur in Twka2, namely, *Dilophodon minusculus* and *Triplopus cubitalis* (McCarroll et al., 1996b), are currently unknown. However, in *T. obliquidens*, which is known from the Uinta B and C horizons in the Uinta Basin (Prothero, 1996), the astragalar neck is not quite as short as in FMNH PM 62461 (Osborn, 1890:pl. 9, fig. 9). While the precise taxonomic identity of FMNH PM 62461 is obscure, it nevertheless reveals the presence of a very small ceratomorph in the Twka3 mammalian assemblage.

DISCUSSION

To date, a total of 12 FMNH localities in the upper unit of the Adobe Town Member (Twka3) have produced 199 catalogued vertebrate specimens. They include 47 mammal specimens from seven localities, of which 16 specimens from six localities that are sufficiently taxonomically identifiable are reported in this paper. The currently known temporal distributions of the taxa reported here from Twka3 are most consistent with an early to middle Uintan (Ui1b–Ui2) age for at least the lower part of the unit, i.e., approximately Roehler's (1973) beds 677–688 (Table 2). Based on the results presented here, we agree with McCarroll et al. (1996a) that the initially hypothesized correlation with the Uinta C horizon (Roehler, 1973; Turnbull, 1972) was in error for at least the lower beds of Twka3 (beds 676–688)

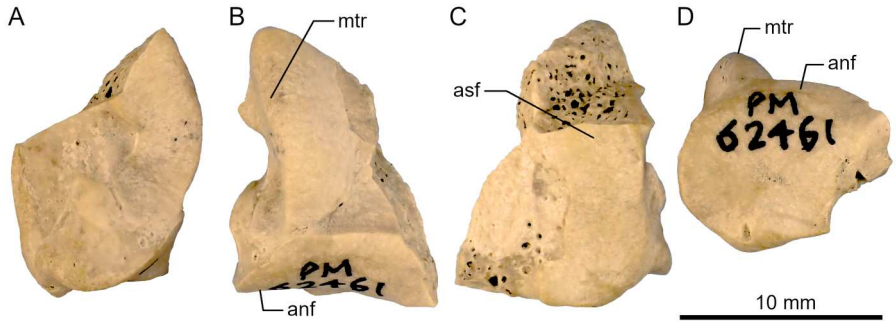

FIGURE 13. Ceratomorpha gen. et sp. indet. Specimen FMNH PM 62461: partial left astragalus in medial, **A**, dorsal, **B**, plantar, **C**, and distal, **D** views. **Abbreviations**: **anf**, astragalar navicular facet; **asf**, astragalar sustentacular facet; **mtr**, medial trochlear ridge.

TABLE 2. Temporal distributions of mammalian taxa from Twka3 outside of Twka3. [a]"*Paramys compressidens*" of McCarroll et al. (1996a). [b]"*Pareumys grangeri*" of McCarroll et al. (1996a), renamed to a new species by Korth (2020). [c]Assumed range-through occurrence; not known from Ui1a-age deposits (cf. Murphey et al., 2018). [d]Undescribed specimens from Twka2 (see main text). [e]Occurrence in southern California based on undescribed specimen (Zack, 2023). [f]Occurrence in Twka2 based on undescribed specimen, FMNH PM 3232. [g]Undescribed specimens from Twka2 (see main text) and a possible Ui-1b portion of Washakie Formation in Sand Wash Basin, Colorado (Dunn, 2024). [h]"*Limnocyon*? sp." of Gazin (1956) and Dawson (1980) from Wagon Bed Formation, Wyoming, and "*Limnocyon* sp." of Walsh (1996) from Santiago Formation, California, which may pertain to *L. potens.*

	Br3	Ui1a	Ui1b	Ui2	Ui3	Du
Above bed 688						
Limnocyon potens			●	●	?[h]	
~beds 677–688						
Pantolestes longicaudus	●	–[c]	●[d]	●	●	
Simidectes			●[e]	●	●	●
Mesomeryx grangeri			●[f]	●		
Epihippus gracilis		●	●	●	●	
Amynodon advenus			●	●	●	
Ourayia uintensis			●[g]	●		
Metaparamys compressidens[a]			●	●	●	
Pareumys flynni[b]	●	–[c]	●			

and potentially the upper beds (689–708) as well. Intense collecting effort has failed to produce enough fossils that could assist in separately assigning a biochron to those upper Twka3 beds.

We rely only on the known fauna for assigning an age to the upper unit of the Adobe Town Member. With the possible exception of *Ourayia uintensis*, the Twka3 assemblage lacks an index species of any Uintan biochron. Of the nine mammalian taxa from Twka3 that are identified at the genus or species level, eight or nine (depending on the age of the Sand Wash Basin locality that has yielded *O. uintensis*) occur in Ui1b-age deposits, including within the underlying Twka2, while eight occur in Ui2-age deposits (Table 2). The support for a Ui1b-age would be reduced slightly if the specimen of *Simidectes* from Twka3 belongs to a different species from the one that occurs in the Friars Formation of southern California (there are no other Ui1b records of the genus)—a likely case considering both the species-level differentiation of Uintan mammalian assemblages in the two regions (cf. Atwater & Kirk, 2018; Gunnell et al., 2009; Tomiya, 2013; Walsh, 1996) and the fact that the astragalus from Twka3 is compatible with *S. medius* in size, while the San Diego specimen is substantially smaller. Thus, the mammalian assemblage of Twka3 is similarly compatible with either Ui1b or Ui2 ages, given the current state of biostratigraphy. In contrast, a late Uintan (Ui3) age for Twka3 is unlikely, as it would require range extensions for three to four taxa (*Mesomeryx grangeri*, *O. uintensis, P. flynni*, and possibly *Limnocyon potens*) that are currently not supported by the dense mammalian fossil record of that age in the Uinta Basin and elsewhere in the central Rocky Mountain region (cf. Gunnell et al., 2009; Robinson et al., 2004). This inference is based on a principle of parsimony, that is, minimizing inter-biochron range extensions within (as in the case of *P. flynni*, whose occurrences are otherwise restricted to Br3–Ui1b portions of the Washakie Formation) as well as among geologic formations.

The difficulty of biochron determination for Twka3 (i.e., assigning a Ui1b versus Ui2 age) is attributable to the still very small number of identifiable specimens ($N = 16$ in this paper), but it also hints at an intermediate stage of mammalian faunal transition that is not captured by the fossil records of the underlying Twka2—a reference section for biochron Ui1b (Gunnell et al., 2009)—or the Uinta Formation. Indeed, the apparent absence of the cylindrodontid rodent *Pareumys flynni* from the Uinta Formation, which has yielded abundant fossil material of congeneric *P. grangeri* (Korth, 2020; Rasmussen et al., 1999), may reflect an older age of Twka3 than the Ui2-age horizons of the Uinta Formation. We anticipate the faunal gap between the presently-recognized biochrons Ui1b and Ui2 to be reduced with additional taxonomic studies of fossil mammals from Twka2, the majority of which have yet to be described in detail (Tomiya et al., 2021).

The mammalian fossil assemblage of Twka3, though still small in sample size, gains paleontological importance as it increases the resolution of the faunal succession data in the region during a period of environmental instability that paved the way for 'modernization' of mammals at the familial level (cf. Black & Dawson, 1966). Here we briefly consider the local environmental history across the Twka2/Twka3 boundary. The upper portion of Twka2 that is unambiguously Ui1b in age (i.e., bed 633 and above; Tomiya et al., 2021) is characterized by:

1) Extreme scarcity of strictly arboreal and semi-aquatic mammals: In the FMNH collection, only a single primate specimen (arboreal) and two specimens of *Pantolestes* (semi-aquatic) are securely known from this interval, compared with 139 rodent specimens (here we use rodents as a standard for comparing relative abundance because they substantially overlap with omomyids and *Pantolestes* in body size but generally do not exhibit strictly arboreal or semi-aquatic locomotor adaptations in the middle Eocene of North America [cf. Anderson, 2008, and references therein; Dunn & Rasmussen, 2007; Matthew, 1910; Turnbull, 1991; Walsh & Storer, 2008]);
2) Absence of *Hyopsodus*;
3) A low diversity of carnivores; and
4) Presence of a ricochetal rodent, *Protoptychus*, which has been interpreted to indicate an "arid or semiarid environment" (Turnbull, 1991:1).

These patterns are in stark contrast to those seen in the Br3-age mammal assemblage from Twka1, and point to a major shift toward a more open (i.e., less forested) environment across the Bridgerian/Uintan boundary in the Washakie Basin (Tomiya et al., 2021). This inferred local transition is broadly congruent with the gradual contraction of the lake systems in the Central Rocky Mountain region from ca. 50 to 45 Ma (Smith et al., 2008) and associated faunal distinctions that have long been recognized among depositional basins of different ages (Gazin, 1955, 1968; Townsend et al., 2010). The mammalian assemblage from Twka3 resembles the Ui1b-age assemblage from Twka2 in the absence of *Hyopsodus*, but there are notable differences. Of particular interest from the paleoenvironmental perspective are the occurrences in Twka3 of an omomyid primate, which was likely an arboreal leaper (cf. Dunn et al., 2006; Dunn, 2010; Monclús-Gonzalo et al., 2025), and of the probably semiaquatic pantolestid *Pantolestes* (cf. Dunn & Townsend 2019). Together, they suggest the presence of at least patches of wooded environment surrounding substantial bodies of water. The specimen counts for the primates ($N = 2$) and *Pantolestes* ($N = 1$) relative to rodents ($N = 3$), and the fact that these two taxa were recovered at all in such a small sample from Twka3, are remarkable in view of their near-absence in the far better-sampled Ui1b-age assemblages from Twka2. Such a composition might reflect a temporary reversal of the regional environmental trend in the Washakie Basin sometime between or within biochrons Ui1b and Ui2, although Uintan primates never regained the Bridgerian-level of abundance in the central Rocky Mountain region (Williams & Kirk, 2008). Collecting of fossils from relatively small and generally fossil-poor exposures of Twka3 has been hampered largely by the steep

topography of the outcrops and difficulty of accessing them. Nevertheless, additional collecting efforts, in combination with analyses of other vertebrate taxa and geologic data, could enable us to test the above hypothesis.

ACKNOWLEDGMENTS

We thank: W. Simpson, K. Angielczyk, and A. Stroup (FMNH) and S. Davis and L. Church (CM) for access to collections under their care and curatorial support; P. Holroyd (University of California Museum of Paleontology), editors of JVP, and two anonymous reviewers for helpful comments on early drafts of this paper; W. Simpson for photographing FMNH PM 61725 and FMNH PM 61739; N. Toyoda (Center for the Evolutionary Origins of Human Behavior, Kyoto University) for help with digital 3D modeling of XCT data; E. Zeiger (FMNH) for typing and proofing early drafts of the manuscript; and M. Alvey (FMNH) for administrative and logistical assistance. J. Alroy (then at the University of Chicago) gave advice on rodent taxonomy, and M. Dawson (CM) and W. Korth (Rochester Institute of Vertebrate Paleontology) assisted with rodent identifications. The Field Museum Department of Geology and the Bureau of Land Management (BLM) supported fieldwork by J.J.F., S.M., and W.D.T, including through BLM permit 213-WY-94. The Paleontological Society, Society for Sedimentary Geology, and University of Chicago Department of the Geophysical Sciences supported fieldwork conducted by M.C.W. under BLM permit PA21-WY-285. U.S. National Science Foundation Collections in Support of Biological Research grant DBI-1203530 (to K. Angielczyk) supported reorganization and expansion of the Washakie Formation fossil collections at FMNH, thereby facilitating the present study. JSPS KAKENHI Grant Number JP22KK0048 (to S.T.) supported the most recent phase of this research. We acknowledge the Field Museum XCT Lab (RRID:SCR_026255) and lab manager S.M. Smith for providing us with the XCT data for the present study.

AUTHOR CONTRIBUTIONS

S.M.M., W.D.T., and J.J.F. (with FMNH field teams) collected the fossil specimens described herein, conducted initial analyses, and wrote early drafts of the manuscript. S.T., R.H.D., S.P.Z., M.C.W., B.B., and J.J.F. reanalyzed the data and revised the manuscript.

DATA AVAILABILITY STATEMENT

The authors confirm that the data supporting the findings of this study are available within the article. The reconstructed XCT slices of selected specimens and the digital 3D models derived from them are deposited on MorphoSource under Project 000774772: "Eocene mammals from Washakie Formation (Wyoming, USA)" (https://www.morphosource.org/projects/000774772/about?locale=en), with the following links:

FMNH PM 56654 (*Ourayia uintensis*): https://n2t.net/ark:/87602/m4/775279 (reconstructed XCT slices); https://n2t.net/ark:/87602/m4/775282 (3D model)

FMNH PM 56655 (*Ourayia uintensis*): https://n2t.net/ark:/87602/m4/775287 (reconstructed XCT slices); https://n2t.net/ark:/87602/m4/775290 (3D model)

FMNH PM 55361 (*Metaparamys compressidens*): https://n2t.net/ark:/87602/m4/775264 (reconstructed XCT slices); https://n2t.net/ark:/87602/m4/775268 (3D model of p4); https://n2t.net/ark:/87602/m4/775271 (3D model of m1); https://n2t.net/ark:/87602/m4/775274 (3D model of m2)

FMNH PM 55060 (*Pareumys flynni*): https://n2t.net/ark:/87602/m4/775305 (reconstructed XCT slices); https://n2t.net/ark:/87602/m4/775311 (3D model of right dentary); https://n2t.net/ark:/87602/m4/775308 (3D model of left dentary)

FMNH PM 56652 (*Mesomeryx* cf. *M. grangeri*): https://n2t.net/ark:/87602/m4/775296 (reconstructed XCT slices); https://n2t.net/ark:/87602/m4/775299 (3D model)

FMNH PM 55311 (*Epihippus gracilis*): https://n2t.net/ark:/87602/m4/776160 (reconstructed XCT slices); https://n2t.net/ark:/87602/m4/776163 (3D model of left dentary); https://n2t.net/ark:/87602/m4/776166 (3D model of left dp2)

DISCLOSURE STATEMENT

No potential conflict of interest was reported by the author(s).

ORCID

Susumu Tomiya http://orcid.org/0000-0001-6038-899X
Rachel H. Dunn http://orcid.org/0000-0002-1647-2796
Shawn P. Zack http://orcid.org/0000-0003-3098-7494
Melissa C. Wood http://orcid.org/0009-0007-2213-165X
Bin Bai http://orcid.org/0000-0003-4394-8689
John J. Flynn http://orcid.org/0000-0003-4705-3591

SUPPLEMENTARY FILES

Supplementary material: Figure S1, comparison of m3s of *Ourayia uintensis* in occlusal (top) and buccal (bottom) views; Figure S2, comparison of m2s of *Ourayia uintensis* in occlusal (top) and buccal (bottom) views; Figure S3, digital 3D models of FMNH PM 55311.

LITERATURE CITED

Alston, E. R. (1876). On the classification of the order Glires. *Proceedings of the Scientific Meetings of the Zoological Society of London for the Year 1876*, 61–98.

Anderson, D. K. (2008). Ischyromyidae. In C. M. Janis, G. F. Gunnell, & M. D. Uhen (Eds.), *Evolution of Tertiary Mammals of North America, Vol. 2: small mammals, xenarthrans, and marine mammals* (pp. 311–325). Cambridge University Press.

Atwater, A. L., & Kirk, E. C. (2018). New middle Eocene omomyines (Primates, Haplorhini) from San Diego County, California. *Journal of Human Evolution*, *124*, 7–24. doi:10.1016/j.jhevol.2018.04.010

Bai, B., Meng, J., Zhang, C., Gong, Y.-X., & Wang, Y.-Q. (2020). The origin of Rhinocerotoidea and phylogeny of Ceratomorpha (Mammalia, Perissodactyla). *Communications Biology*, *3*(1), 1–16. doi:10.1038/s42003-019-0734-6

Black, C. C., & d Dawson, M. R. (1966). A review of late Eocene mammalian faunas from North America. *American Journal of Science*, *264*(5), 321–349. doi:10.2475/ajs.264.5.321

Bowdich, T. E. (1821). *Analysis of the natural classifications of Mammalia for the use of students and travellers*. J. Smith.

Bryant, H. N. (1996). Explicitness, stability, and universality in the phylogenetic definition and usage of taxon names: a case study of the phylogenetic taxonomy of the Carnivora (Mammalia). *Systematic Biology*, *45*(2), 174–189. doi:10.1093/sysbio/45.2.174

Clark, J. (1939). *Miacis gracilis*, a new carnivore from the Uinta Eocene. *Annals of the Carnegie Museum*, *27*, 349–370. doi:10.5962/p.214440

Clark, J. (1941). An anaptomorphid primate from the Oligocene of Montana. *Journal of Paleontology*, *15*, 562–563.

Colbert, M. W. (2006a). *Hesperaletes* (Mammalia: Perissodactyla), a new tapiroid from the middle Eocene of southern California. *Journal of Vertebrate Paleontology*, *26*(3), 697–711. doi:10.1671/0272-4634(2006)26[697:HMPANT]2.0.CO;2

Colbert, M. W. (2006b). Variation and species recognition in Eocene tapirs from Southern California. *Journal of Vertebrate Paleontology*, *26*(3), 712–719. doi:10.1671/0272-4634(2006)26[712:VASRIE]2.0.CO;2

Coombs, M. C. (1971). Status of *Simidectes* (Insectivora, Pantolestoidea) of the late Eocene of North America. *American Museum Novitates*, *2455*, 1–41.

Cope, E. D. (1872). Second account of new Vertebrata from the Bridger Eocene. *Proceedings of the American Philosophical Society*, *12*, 466–468.

Cope, E. D. (1884). The Vertebrata of the Tertiary formations of the West. *Report of the United States Geological Survey of the Territories*, *3*, 1–1009.

Covey, D., & McCarroll, S. M. (1996). The artiodactyl fauna of the Washakie Formation, Eocene age, of southern Wyoming. *Journal of Vertebrate Paleontology*, *16*, 29A.

Dawson, M. R. (1980). Paleontology and geology of the Badwater Creek area, central Wyoming, Part 20: the late Eocene Creodonta and Carnivora. *Annals of the Carnegie Museum*, *49*, 79–91. doi:10.5962/p.330838

Dunn, R. H. (2010). Additional postcranial remains of omomyid primates from the Uinta Formation, Utah and implications for the locomotor behavior of large-bodied omomyids. *Journal of human evolution*, *58*(5), 406–417. doi:10.1016/j.jhevol.2010.02.010

Dunn, R. H. (2024). New primates from the middle Eocene of the Sand Wash Basin, northwestern Colorado. *Journal of Human Evolution*, *197*, 103612. doi:10.1016/j.jhevol.2024.103612

Dunn, R. H., & Rasmussen, D. T. (2007). Skeletal morphology and locomotor behavior of *Pseudotomus eugenei* (Rodentia, Paramyinae) from the Uinta Formation, Utah. *Journal of Vertebrate Paleontology*, *27*(4), 987–1006. doi:10.1671/0272-4634(2007)27[987:SMALBO]2.0.CO;2

Dunn, R. H., Sybalsky, J. M., Conroy, G. C., & Rasmussen, D. T. (2006). Hindlimb adaptations in *Ourayia* and *Chipetaia*, relatively large-bodied omomyine primates from the middle Eocene of Utah. *American Journal of Physical Anthropology*, *131*(3), 303–310. doi:10.1002/ajpa.20407

Dunn, R. H., & Townsend, K. E. B. (2019). New pantolestids from the Uinta Formation, Utah. *Journal of Vertebrate Paleontology*, *39*(4), e1652622. doi:10.1080/02724634.2019.1652622

Flynn, J. J. (1986). Correlation and geochronology of middle Eocene strata from the western United States. *Palaeogeography, Palaeoclimatology, Palaeoecology*, *55*(2-4), 335–406. doi:10.1016/0031-0182(86)90155-0

Flynn, J. J., Finarelli, J., & Spaulding, M. (2010). Phylogeny of the Carnivora and Carnivoramorpha, and the use of the fossil record to enhance understanding of evolutionary transformations. In A. Goswami, & A. R. Friscia (Eds.), *Carnivoran Evolution: new views on phylogeny, form, and function* (pp. 25–63). Cambridge University Press, Cambridge. doi:10.1017/CBO9781139193436.003

Flynn, J. J., Wyss, A. R., & Wolsan, M. (2020). Pan-Carnivora. In K. de Queiroz, P. Cantino, & J. A. Gauthier (Eds.), *Phylonyms: a companion to the PhyloCode* (pp. 979–982). CRC Press, Boca Raton. doi:10.1201/9780429446276

Froehlich, D. J. (1999). Phylogenetic systematics of basal perissodactyls. *Journal of Vertebrate Paleontology*, *19*(1), 140–159. doi:10.1080/02724634.1999.10011129

Froehlich, D. J. (2002). Quo vadis eohippus? The systematics and taxonomy of the early Eocene equids (Perissodactyla). *Zoological Journal of the Linnean Society*, *134*(2), 141–256. doi:10.1046/j.1096-3642.2002.00005.x

Gazin, C. L. (1955). A review of the upper Eocene Artiodactyla of North America. *Smithsonian Miscellaneous Collections*, *128*, 1–96.

Gazin, C. L. (1956). The geology and vertebrate paleontology of upper Eocene strata in the northeastern part of the Wind River Basin, Wyoming, Part 2: the mammalian fauna of the Badwater Area. *Smithsonian Miscellaneous Collections*, *131*, 1–35.

Gazin, C. L. (1958). A review of the middle and upper Eocene primates of North America. *Smithsonian Miscellaneous Collections*, *136*, 1–112.

Gazin, C. L. (1968). A study of the Eocene condylarthran mammal *Hyopsodus*. *Smithsonian Miscellaneous Collections*, *153*, 1–90.

Geisler, J. H. (2001). New morphological evidence for the phylogeny of Artiodactyla, Cetacea, and Mesonychidae. *American Museum Novitates*, *3344*, 1–53. doi:10.1206/0003-0082(2001)344<0001:NMEftp>2.0.CO;2

Golz, D. J., & Lillegraven, J. (1977). Summary of known occurrences of terrestrial vertebrates from Eocene strata of southern California. *Rocky Mountain Geology*, *15*, 43–65.

Granger, W. (1908). A revision of the American Eocene horses. *Bulletin of the American Museum of Natural History*, *24*, 221–264.

Granger, W. (1909). Faunal horizons of the Washakie Formation of southern Wyoming. *Bulletin of the American Museum of Natural History*, *26*, 13–23.

Gray, J. E. (1821). On the natural arrangement of vertebrose animals. *London Medical Repository*, *15*, 296–310.

Gunnell, G. (1998). Creodonta. In C. M. Janis, K. M. Scott, & L. L. Jacobs (Eds.), *Evolution of Tertiary Mammals of North America, Vol. 1: terrestrial carnivores, ungulates, and ungulatelike mammals* (pp. 91–109). Cambridge University Press.

Gunnell, G. F., Murphey, P. C., Stucky, R. K., Townsend, K. B., Robinson, P., Zonneveld, J., Bartels, W., & Albright, L. (2009). Biostratigraphy and biochronology of the latest Wasatchian, Bridgerian, and Uintan North American land mammal "ages.". *Museum of Northern Arizona Bulletin*, *65*, 279–330.

Gustafson, E. P. (1979). Early Tertiary vertebrate faunas Big Bend Area Trans-Pecos Texas: *Simidectes* (Mammalia, Insectivora). *Pearce-Sellards Series*, *31*, 1–9.

Haeckel, E. (1866). *Generelle Morphologie der Organismen, Allgemeine Grundzüge der organischen Formen-Wissenschaft, mechanisch begründet durch die von Charles Darwin reformierte Descendenz-Theorie, Band 2: Allgemeine Entwicklungsgeschichte der Organismen*. Georg Reimer.

Hooker, J. J. (2005). Perissodactyla. In K. Rose, & J. J. Archibald (Eds.), *The Rise of Placental Mammals: origins and relationships of the major extant clades* (pp. 199–214). Johns Hopkins University Press.

Kay, J. L. (1957). The Eocene vertebrates of the Uinta Basin, Utah. In O. G. Seal (Ed.), *Guidebook to the Geology of the Uinta Basin, 8th Annual Field Conference* (pp. 110–114). Intermountain Association of Petroleum Geologists.

Kelly, T. S., & Murphey, P. C. (2016). Mammals from the earliest Uintan (middle Eocene) Turtle Bluff Member, Bridger Formation, southwestern Wyoming, USA, Part 1: Primates and Rodentia. *Palaeontologia Electronica*, *19.2.27A*, 1–55. doi:10.26879/586

Kirk, E. C., Dunn, R. H., Rodwell, B., & Townsend, K. B. (2023). New specimens of middle Eocene omomyines (Primates, Omomyoidea) from the Uinta Basin of Utah and the Tornillo Basin of Texas, with clarification of the generic status of *Ourayia*, *Mytonius*, and *Diablomomys*. *Journal of Human Evolution*, *183*, 103425. doi:10.1016/j.jhevol.2023.103425

Korth, W. W. (1988). *Paramys compressidens* Peterson and the systematic relationships of the species of *Paramys* (Paramyinae, Ischyromyidae). *Journal of Paleontology*, *62*(3), 468–471. doi:10.1017/S0022336000059266

Korth, W. W. (2020). New material of fossil rodents (Mammalia) from the Eocene (Bridgerian-Uintan) Washakie Formation, southcentral Wyoming. *Proceedings of the Biological Society of Washington*, *133*(1), 18–34. doi:10.2988/19-00011

Korth, W. W., & Emry, R. J. (2007). A new genus of paramyine (Ischyromyidae, Rodentia) from the Eocene (Uintan to Chadronian) of Wyoming and Utah. *Bulletin of Carnegie Museum of Natural History*, *39*, 151–155. doi:10.2992/0145-9058(2007)39[151:ANGOPI]2.0.CO;2

Krishtalka, L., Stucky, R. K., West, R. M., McKenna, M. C., Black, C. C., Bown, Dawson, M. R., Golz, D. J., Flynn, J. J., Lillegraven, J. A., & Turnbull, W. D. (1987). Eocene (Wasatchian through Duchesnean) biochronology of North America. In M. O. Woodburne (Ed.), *Cenozoic Mammals of North America: geochronology and biochronology* (pp. 77–117). University of California Press, Berkeley.

Leidy, J. (1869a). Notice of some extinct vertebrates from Wyoming and Dakota. *Proceedings of the Academy of Natural Sciences of Philadelphia [Year 1869]*, 63–67.

Leidy, J. (1869b). The extinct mammalian fauna of Dakota and Nebraska including an account of some allied forms from other localities, together with a synopsis of the mammalian remains of North America. *Journal of the Academy of Natural Sciences of Philadelphia (2nd ser.)*, *7*, 1–472.

Leidy, J. (1873). Contributions to the extinct vertebrate fauna of the western territories. *Report of the United States Geological Survey of the Territories*, *1*, 1–358.

Linnaeus, C. (1758). *Systema Naturae Per Regna Tria Naturae, Secundum Classes, Ordines, Genera, Species, cum Characteribus, Diferentiis, Synonymis, Locis, Tomus I: Editio decima, reformata*. Laurentii Salvii.

Love, J. D., & Christiansen, A. C. (1985). *Geologic map of Wyoming*. US Geological Survey.

Maas, M., Hussain, S., Leinders, J., & Thewissen, J. (2001). A new isectolophid tapiromorph (Perissodactyla, Mammalia) from the Early Eocene of Pakistan. *Journal of Paleontology*, *75*(2), 407–417. doi:10.1666/0022-3360(2001)075<0407:ANITPM>2.0.CO;2

MacFadden, B. J. (1976). Cladistic analysis of primitive equids, with notes on other perissodactyls. *Systematic Zoology*, *25*(1), 1–14. doi:10.2307/2412774

MacFadden, B. J. (1998). Equidae. In C. M. Janis, K. M. Scott, & L. L. Jacobs (Eds.), *Evolution of Tertiary Mammals of North America, Vol. 1: terrestrial carnivores, ungulates, and ungulatelike mammals* (pp. 537–559). Cambridge University Press.

Marsh, O. C. (1871). Notice of some new fossil mammals from the Tertiary formation. *American Journal of Science (3rd ser.)*, *3*(7), 35–44. doi:10.2475/ajs.s3-2.7.35

Marsh, O. C. (1872a). Preliminary description of new Tertiary mammals, Part 1. *American Journal of Science (3rd ser.)*, *4*, 122–128. doi:10.2475/ajs.s3-4.20.122

Marsh, O. C. (1872b). Preliminary description of new Tertiary mammals, Part 2–3. *American Journal of Science (3rd ser.)*, *4*, 202–224. doi:10.2475/ajs.s3-4.21.202

Marsh, O. C. (1875). Notice of new Tertiary mammals, IV. *American Journal of Science (3rd ser.)*, *9*(51), 239–250. doi:10.2475/ajs.s3-9.51.239

Marsh, O. C. (1877). Notice of some new vertebrate fossils. *American Journal of Science (3rd ser.)*, *14*(81), 249–256. doi:10.2475/ajs.s3-14.81.249

Marsh, O. C. (1878). Introduction and succession of vertebrate life in America. *Popular Science Monthly*, *12*, 672–697.

Marsh, O. C. (1894). Description of Tertiary Artiodactyles. *American Journal of Science (3rd ser.)*, *48*(285), 259–274. doi:10.2475/ajs.s3-48.285.259

Martinez, J., & Sudre, J. (1995). The astragalus of Paleogene artiodactyls: comparative morphology, variability and prediction of body mass. *Lethaia*, *28*(3), 197–209. doi:10.1111/j.1502-3931.1995.tb01423.x

Matthew, W. D. (1909). The Carnivora and Insectivora of the Bridger Basin, middle Eocene. *Memoirs of the American Museum of Natural History*, *9*, 289–576.

Matthew, W. D. (1910). On the osteology and relationships of *Paramys*, and the affinities of the Ischyromyidae. *Bulletin American Museum of Natural History*, *38*, 43–72.

Matthew, W. D., & Granger, W. (1925). New mammals from the Irdin Manha Eocene of Mongolia. *American Museum Novitates*, *198*, 1–10.

McCarroll, S. M. (1995). An early Uintan fauna from the upper unit of the Adobe Town Member, Washakie Formation, Washakie Basin, Wyoming. *Journal of Vertebrate Paleontology*, *15*, 42A.

McCarroll, S. M., Flynn, J. J., & Turnbull, W. D. (1996a). Biostratigraphy and magnetostratigraphy of the Bridgerian-Uintan Washakie Formation, Washakie Basin, Wyoming. In D. R. Prothero, & R. J. Emry (Eds.), *The Terrestrial Eocene–Oligocene Transition in North America* (pp. 25–39). Cambridge University Press.

McCarroll, S. M., Flynn, J. J., & Turnbull, W. D. (1996b). The mammalian faunas of the Washakie Formation, Eocene age, of southern Wyoming, Part III: the perissodactyls. *Fieldiana Geology (new series)*, *33*, 1–38.

McGrew, P. O. (1953). A new and primitive early Oligocene horse from Trans-Pecos Texas. *Fieldiana Geology*, *10*, 167–171.

McKenna, M. C. (1975). Toward a phylogenetic classification of the Mammalia. In W. P. Luckett, & F. S. Szalay (Eds.), *Phylogeny of the primates: a multidisciplinary approach* (pp. 21–46). Plenum Press.

Miller, G. S., & Gidley, J. W. (1918). Synopsis of the supergeneric groups of rodents. *Journal of the Washington Academy of Sciences*, *8*, 431–448.

Monclús-Gonzalo, O., Alba, D. M., Fabre, A. C., & Marigó, J. (2025). Reconstruction of the locomotor repertoire of early primates in the light of astragalar and calcaneal shape. *Journal of Human Evolution*, *206*, 103730. doi:10.1016/j.jhevol.2025.103730

Murphey, P. C., & Dunn, R. H. (2009). *Hemiacodon engardae*, a new species of omomyid primate from the earliest Uintan Turtle Bluff Member of the Bridger Formation, southwestern Wyoming, USA. *Journal of Human Evolution*, *57*, 123–130. doi:10.1016/j.jhevol.2009.05.006

Murphey, P. C., & Kelly, T. S. (2017). Mammals from the earliest Uintan (middle Eocene) Turtle Bluff Member, Bridger Formation, southwestern Wyoming, USA, Part 2: Apatotheria, Lipotyphla, Carnivoramorpha, Condylartha, Dinocerata, Perissodactyla and Artiodactyla. *Palaeontologia Electronica*, *20.1.29A*, 1–51. doi:10.26879/720

Murphey, P. C., Kelly, T. S., Chamberlain, K. R., Tsukui, K., & Clyde, W. C. (2018). Mammals from the earliest Uintan (middle Eocene) Turtle Bluff Member, Bridger Formation, southwestern Wyoming, USA, Part 3: Marsupialia and a reevaluation of the Bridgerian-Uintan North American Land Mammal Age transition. *Palaeontologia Electronica*, *21.2.25A*, 1–52. doi:10.26879/804

Osborn, H. F. (1890). The Mammalia of the Uinta formation, Part 3: Perissodactyla. *Transactions of the American Philosophical Society*, *16*, 505–530.

Osborn, H. F. (1895). Fossil mammals of the Uinta Basin: expedition of 1894. *Bulletin of the American Museum of Natural History*, *7*, 71–105.

Osborn, H. F. (1913). *Eomoropus*, an American Eocene chalicothere. *Bulletin of the American Museum of Natural History*, *32*, 261–274.

Owen, R. (1848). Description of teeth and portions of jaws of two extinct anthracotherioid quadrupeds (*Hyopotamus vectianus* and *Hyop. bovinus*) discovered by the Marchioness of Hastings in the Eocene deposits on the NW coast of the Isle of Wight: with an attempt to develope Cuvier's idea of the classification of pachyderms by the number of their toes. *Quarterly Journal of the Geological Society of London*, *4*, 103–141.

Peterson, O. A. (1919). Report upon the material discovered in the upper Eocene of the Uinta Basin by Earl Douglas in the years 1908-1909, and by O.A. Peterson in 1912. *Annals of the Carnegie Museum*, *12*, 40–169.

Prothero, D. R. (1996). Magnetic stratigraphy and biostratigraphy of the middle Eocene Uinta Formation, Uinta Basin, Utah. In D. R. Prothero, & R. J. Emry (Eds.), *The Terrestrial Eocene-Oligocene Transition in North America* (pp. 3–24). Cambridge University Press.

Radinsky, L. B. (1965). Early Tertiary Tapiroidea of Asia. *Bulletin of the American Museum of Natural History*, *129*, 181–264.

Radinsky, L. B. (1966). The adaptive radiation of the phenacodontid condylarths and the origin of the Perissodactyla. *Evolution*, *20*, 408–417.

Rasmussen, D. T., Conroy, G. C., Friscia, A. R., Townsend, K. E., & Kinkel, M. D. (1999). Mammals of the middle Eocene Uinta Formation. In D. D. Gillette (Ed.), *Vertebrate Paleontology in Utah (Utah Geological Survey Miscellaneous Publication 99-1)* (pp. 401–420). Utah Geological Survey.

Robinson, P. (1968). The paleontology and geology of the Badwater Creek area, central Wyoming, Part 4: Late Eocene primates from Badwater, Wyoming, with a discussion of material from Utah. *Annals of Carnegie Museum*, *39*, 307–326.

Robinson, P., Gunnell, G. F., Walsh, S. L., Clyde, W. C., Storer, J. E., Stucky, R. K., Froehlich, D. J., Ferrusquia-Villafranca, I., & McKenna, M. C. (2004). Wasatchian through Duchesnean biochronology. In M. O. Woodburne (Ed.), *Late Cretaceous and Cenozoic mammals of North America: biostratigraphy and geochronology* (pp. 106–155). Columbia University Press.

Roehler, H. W. (1973). Stratigraphy of the Washakie Formation in the Washakie basin, Wyoming. *Geological Survey Bulletin*, *1369*, 1–40.

Roehler, H. W. (1985). *Geologic map of the Kinney Rim 30 (60 minute quadrangle, Wyoming and Colorado*. IMAP 1615. US Geological Survey.

Roehler, H. W. (1992). Description and correlation of Eocene rocks in stratigraphic reference sections for the Green River and Washakie basins, southwest Wyoming. *U.S. Geological Survey Professional Paper*, *1506-D*, D1–D83.

Rose, K. D., Holbrook, L. T., & Luckett, W. P. (2018). Deciduous premolars of Eocene Equidae and their phylogenetic significance. *Historical Biology*, *30*, 89–118. doi:10.1080/08912963.2017.1291637

Scott, J., Sutherland, W., Johnson, J., & McLaughlin, J. (2011). *Geologic map of the Baggs 30' x 60' quadrangle, Carbon and Sweetwater counties, Wyoming, and Moffat and Routt counties, Colorado. Map Series 95*. Wyoming State Geological Survey.

Scott, W. B., & Osborn, H. F. (1883). On the skull of the Eocene rhinoceros, *Orthocynodon*, and the relation of this genus to other members of the group. *Bulletin (Contributions from the E. M. Museum of Geology and Archaeology of Princeton College)*, *3*, 1–22.

Smith, M. E., Carroll, A. R., & Singer, B. S. (2008). Synoptic reconstruction of a major ancient lake system: Eocene Green River Formation, western United States. *Geological Society of America Bulletin*, *120*, 54–84. doi:10.1130/B26073.1

Solé, F. (2013). New proviverrine genus from the early Eocene of Europe and the first phylogeny of late Palaeocene–middle Eocene hyaenodontidans (Mammalia). *Journal of Systematic Palaeontology*, *11*, 375–398. doi:10.1080/14772019.2012.686927

Solé, F., Smith, T., De Bast, E., Codrea, V., & Gheerbrant, E. (2016). New carnivoraforms from the latest Paleocene of Europe and their bearing on the origin and radiation of Carnivoraformes (Carnivoramorpha, Mammalia). *Journal of Vertebrate Paleontology*, *36*, e1082480. doi:10.1080/02724634.2016.1082480

Spaulding, M., & Flynn, J. J. (2009). Anatomy of the postcranial skeleton of "*Miacis" uintensis* (Mammalia: Carnivoramorpha). *Journal of Vertebrate Paleontology*, *29*, 1212–1223. doi:10.1671/039.029.0408

Spaulding, M., & Flynn, J. J. (2012). Phylogeny of the Carnivoramorpha: the impact of postcranial characters. *Journal of Systematic Palaeontology*, *10*, 653–677. doi:10.1080/14772019.2011.630681

Stock, C. (1933). A miacid from the Sespe upper Eocene, California. *Proceedings of the National Academy of Sciences*, *19*, 481–486. doi:10.1073/pnas.19.5.481

Stock, C. (1934). New Creodonta from the Sespe Upper Eocene, California. *Proceedings of the National Academy of Sciences*, *20*, 423. doi:10.1073/pnas.20.7.423

Stucky, R. K. (1998). Eocene bunodont and bunoselenodont Artiodactyla. In C. M. Janis, K. M. Scott, & L. L. Jacobs (Eds.), *Evolution of Tertiary Mammals of North America, Vol. 1: terrestrial carnivores, ungulates, and ungulatelike mammals* (pp. 358–374). Cambridge University Press.

Szalay, F. S. (1976). Systematics of the Omomyidae (Tarsiiformes, Primates): taxonomy, phylogeny, and adaptations. *Bulletin of the American Museum of Natural History*, *156*, 157–450.

Theodor, J. M., Erfurt, J., & Métais, G. (2007). The earliest artiodactyls. In D. R. Prothero, & S. E. Foss (Eds.), *The Evolution of Artiodactyls* (pp. 32–58). Johns Hopkins University Press.

Thorpe, M. R. (1923). New species of Uinta Carnivora from White River, Utah. *American Journal of Science*, *5*, 218–224. doi:10.2475/ajs.s5-5.27.218

Tomiya, S. (2012). *Ecological Aspects of the Diversity Dynamics of North American Fossil Mammals*. Ph.D. dissertation, University of California, Berkeley, Berkeley. https://escholarship.org/uc/item/6973872f.

Tomiya, S. (2013). New carnivoraforms (Mammalia) from the middle Eocene of California, USA, and comments on the taxonomic status of '*Miacis' gracilis*. *Palaeontologia Electronica*, *16.2.14A*, 1–29. doi:10.26879/364

Tomiya, S., Zack, S. P., Spaulding, M., & Flynn, J. J. (2021). Carnivorous mammals from the middle Eocene Washakie Formation, Wyoming, USA, and their diversity trajectory in a post-warming world. *Journal of Paleontology 95* (Memoir 82), 1–115. doi:10.1017/jpa.2020.74

Townsend, K. E., Friscia, A. R., & Rasmussen, D. T. (2006). Stratigraphic distribution of upper middle Eocene fossil vertebrate localities in the eastern Uinta Basin, Utah, with comments on Uintan biostratigraphy. *Mountain Geologist*, *43*, 115–134.

Townsend, K. E. B., Rasmussen, D. T., Murphey, P. C., & Evanoff, E. (2010). Middle Eocene habitat shifts in the North American western interior: a case study. *Palaeogeography, Palaeoclimatology, Palaeoecology*, *297*, 144–158. doi:10.1016/j.palaeo.2010.07.024

Trouessart, ÉL. (1879). Catalogue des mammifères vivants et fossiles. *Revue et magasin de zoologie pure et appliquée (Ser. 3)*, *7*, 219–285.

Tsukui, K., & Clyde, W. C. (2012). Fine-tuning the calibration of the early to middle Eocene geomagnetic polarity time scale: paleomagnetism of radioisotopically dated tuffs from Laramide foreland basins. *Geological Society of America Bulletin*, *124*, 870–885. doi:10.1130/B30545.1

Tsukui, K., Flynn, J. J., Hemming, S. R., Ramezani, J., Machlus, M. L., Nuñez, C., McCarroll, S. M., & Bowring, S. A. (2025). Magnetostratigraphy and U-Pb geochronology of the middle Eocene Bridger Formation (Wyoming, USA): Implications for the age and correlation of the Bridgerian/Uintan NALMA boundary and calibration of the Geomagnetic Polarity Time Scale. *Geological Society of America Bulletin*, *137*(7-8), 3463–3480. doi:10.1130/B37223.1

Turnbull, W. (1972). The Washakie Formation of Bridgerian-Uintan ages, and the related faunas. In R. M. West (Ed.), *Guidebook: field conference on Tertiary biostratigraphy of southern and western Wyoming* (pp. 20–31). Department of Biology, Adelphi University.

Turnbull, W. D. (1978). The mammalian faunas of the Washakie Formation, Eocene age, of southern Wyoming, part I: introduction: the geology, history, and setting. *Fieldiana Geology 33* (Publ. 1279), 569–601.

Turnbull, W. D. (1991). *Protoptychus hatcheri* Scott, 1895: the mammalian faunas of the Washakie Formation, Eocene age, of southern Wyoming, part II: the Adobetown Member, middle division (= Washakie B), Twka/2 (in part). *Fieldiana Geology (new series) 21* (Publ. 1421), 1–33.

Van Valen, L. M. (1967). New Paleocene insectivores and insectivore classification. *Bulletin of the American Museum of Natural History*, *135*, 217–284.

Wall, W. P. (1982). The genus *Amynodon* and its relationship to other members of the Amynodontidae (Perissodactyla, Rhinocerotoidea). *Journal of Paleontology*, *56*, 434–443.

Walsh, S. L. (1996). Middle Eocene mammal faunas of San Diego County, California. In D. R. Prothero, & R. J. Emry (Eds.), *The Terrestrial Eocene-Oligocene Transition in North America* (pp. 74–119). Cambridge University Press.

Walsh, S. L., & Storer, J. E. (2008). Cylindrodontidae. In C. M. Janis, G. F. Gunnell, & M. D. Uhen (Eds.), *Evolution of tertiary mammals of North America, Volume 2: small mammals, xenarthrans, and marine mammals* (pp. 336–354). Cambridge University Press.

Wesley, G. D., & Flynn, J. J. (2003). A revision of *Tapocyon* (Carnivoramorpha), including analysis of the first cranial specimens and identification of a new species. *Journal of Paleontology*, *77*, 769–783. doi:10.1666/0022-3360(2003)0772.0.CO;2

Westgate, J. W. (1990). Uintan land mammals (excluding rodents) from an estuarine facies of the Laredo Formation (middle Eocene, Claiborne Group) of Webb County, Texas. *Journal of Paleontology*, *64*, 454–468. doi:10.1017/S0022336000018709

Williams, B. A., & Kirk, E. C. (2008). New Uintan primates from Texas and their implications for North American patterns of species richness during the Eocene. *Journal of Human Evolution*, *55*, 927–941. doi:10.1016/j.jhevol.2008.07.007

Wilson, J. A., & Schiebout, J. A. (1981). Early Tertiary vertebrate faunas, Trans-Pecos Texas: Amynodontidae. *Pearce-Sellards Series*, *33*, 1–62.

Wilson, J. A., & Stevens, M. S. (1986). Fossil vertebrates from the latest Eocene, Skyline channels, Trans-Pecos Texas. In K. M. Flannagan, & J. A. Lillegraven (Eds.), *Vertebrates, Phylogeny, and Philosophy (University of Wyoming Contributions to Geology, Special Paper 3)* (pp. 221–235). University of Wyoming.

Wood, A. E. (1962). The early Tertiary rodents of the family Paramyidae. *Transactions of the American Philosophical Society*, *52*, 1–261.

Wood, H. E., II. (1937). Perissodactyl suborders. *Journal of Mammalogy 18*, 106–106.

Wortman, J. L. (1901). Studies of Eocene Mammalia in the Marsh Collection, Peabody Museum. *American Journal of Science*, *11*, 333–348. 437–450.

Wortman, J. L. (1902). Studies of Eocene Mammalia in the Marsh Collection, Peabody Museum. *American Journal of Science*, *14*, 17–23.

Wortman, J. L., & Matthew, W. D. (1899). The ancestry of certain members of the Canidae, the Viverridae, and Procyonidae. *Bulletin of the American Museum of Natural History*, *12*, 109–139.

Wyss, A. R., & Flynn, J. J. (1993). A phylogenetic analysis and definition of the Carnivora. In F. S. Szalay, M. J. Novacek, & M. C. McKenna (Eds.), *Mammal Phylogeny, vol. 2: Placentals* (pp. 32–52). Springer-Verlag.

Zachos, J., Pagani, M., Sloan, L., Thomas, E., & Billups, K. (2001). Trends, rhythms, and aberrations in global climate 65 Ma to present. *Science*, *292*, 686–693. doi:10.1126/science.1059412

Zack, S. P. (2023). A new species of *Simidectes* from the early Uintan of California clarifies the affinities of the genus. *Journal of Vertebrate Paleontology Program and Abstracts*, *2023*, 464.

Handling Editor: Jonathan Bloch.